Received: 3 December 2020 | Accepted: 7 December 2020

DOI: 10.1002/gea.21840

RESEARCH ARTICLE

Geoarchaeology An International Journal WILEY

Spatial and temporal variability in geomorphic change at tidally influenced shipwreck sites: The use of time-lapse multibeam data for the assessment of site formation processes

Jan Majcher[1] | Rory Quinn[1] | Ruth Plets[1,2] | Mark Coughlan[3,4] | Christopher McGonigle[1] | Fabio Sacchetti[5] | Kieran Westley[1]

[1]School of Geography and Environmental Sciences, University of Ulster, Coleraine, Northern Ireland, UK

[2]Flanders Marine Institute, InnovOcean Site, Oostende, Belgium

[3]School of Civil Engineering, University College Dublin, Dublin, Ireland

[4]Irish Centre for Research in Applied Geosciences, O'Brien Centre for Science East, University College Dublin, Dublin, Ireland

[5]Marine Institute, Oranmore, Ireland

Correspondence

Jan Majcher, School of Geography and Environmental Sciences, University of Ulster, Coleraine, Northern Ireland, BT52 1SA, UK.
Email: majcher-j@ulster.ac.uk

Scientific editing by. Stathis Stiros

Funding information

Ulster University; Marine Institute Ireland

Abstract

Shipwrecks are an integral part of our maritime archaeological landscape and are associated with diverse societal and cultural interests, yielding significant management challenges. Coupled hydrodynamic and geomorphological processes significantly impact the effective in situ preservation of these fragile sites. In this study, we assess sediment budget change and hydrodynamic triggers at metal-hulled shipwrecks lost between 1875 and 1918, all located in the tidally dominated Irish Sea at depths between 26 and 84 m. This is conducted using time-lapse, multibeam echosounder surveys at multi-annual, annual, and weekly time steps, supported by sediment grain-size analysis, modeled ocean currents, and shallow seismic data. Results indicate significant changes at all time steps for sites located in sand-dominated environments, whereas the seabed around shipwrecks settled in multimodal sediments shows virtually no change outside of measurement errors (±30 cm). Variability in geomorphic change is attributed to local environmental factors, including bed shear stress, sediment supply, and spatial barriers to scour. We demonstrate that individual wrecks in similar shelf sea regions can be in very different equilibrium states, which has critical implications for the in situ management of underwater cultural heritage.

KEYWORDS

marine geoarchaeology, seabed geomorphology, sediment transport, shipwreck, site formation processes

1 | INTRODUCTION

Historic shipwrecks are of interest from many different perspectives (Firth, 2018), as objects of cultural heritage and archaeological value (Delgado & Varmer, 2015; Elkin et al., 2020), as hidden pollution sources (Landquist et al., 2013; Vanninen et al., 2020), as habitats for marine life (e.g., Bałazy et al., 2019; Johnson et al., 2020), and as indicators of local oceanographic and seabed morphodynamic conditions (Caston, 1979; Garlan et al., 2015; Geraga et al., 2020). Their preservation state is a result of site formation processes that

comprise various natural and anthropogenic influences (O'Shea, 2002; I. A. K. Ward et al., 1999). Understanding the temporal and spatial nature and scale of these processes is, therefore, critical to their long-term and sustainable management (Frost, 1961; Gregory et al., 2014; Muckelroy, 1978; Pascoe, 2012).

In situ preservation of shipwrecks is encouraged by the UNESCO Convention on the Protection of the Underwater Cultural Heritage, which states that assessments of environmental characteristics should be included in site investigations to examine long-term stability of the underwater cultural heritage (UNESCO, 2002). According to the Convention, these assessments should be conducted without causing disruption to sites, thus promoting the use of non-destructive methods (UNESCO, 2002).

Present-day seabed mapping technology and techniques allow for precise, nonintrusive mapping of underwater archaeological sites with centimetric precision (Ferentinos et al., 2020; Ødegård et al., 2018; Plets et al., 2011; Westley et al., 2011, 2019). It is now possible not only to detect and identify shipwrecks remotely, but also to analyze and quantify geomorphic change at underwater sites through repeat high-resolution multibeam echosounder (MBES) bathymetric surveys (Astley, 2016; Bates et al., 2011; Brennan et al., 2016; Quinn & Boland, 2010; Stieglitz & Waterson, 2013). Moreover, buried parts of shipwrecks and subseabed records of site formation processes can be imaged using shallow seismic techniques (Cvikel et al., 2017; Geraga et al., 2020; Grøn et al., 2015; Plets et al., 2009; Quinn et al., 1997). The use of a combination of these methods allows for a holistic characterization of sites and assessment of their evolution in a time-efficient, noninvasive way (Astley, 2016; Bethencourt et al., 2018; Geraga et al., 2020; Quinn et al., 2007).

Shipwreck sites are often considered as systems in a state of equilibrium achieved sometime after an initial wrecking incident (Astley, 2016; Quinn, 2006; Quinn & Boland, 2010; I. A. K. Ward et al., 1999; Wheeler, 2002). This equilibrium state is dynamic, meaning that it can be perturbed by external or internal forces. This perturbation in the system can result in either a new equilibrium state or maintenance of the current one, depending on the system's capacity to absorb external forces (Astley, 2016; Quinn, 2006; Quinn & Boland, 2010). The dynamics of equilibrium varies across wreck sites, with some subject to disruptions by storms (Fernández-Montblanc et al., 2016, 2018; McNinch et al., 2006), varying tidal currents (Astley, 2016; Quinn & Smyth, 2018), or anthropogenic impacts (Brennan et al., 2013; Gibbs, 2006), whereas others are nearly static, located in more stable physical environments (Eriksson & Rönnby, 2012). What is common is that all wreck sites are characterized by a negative disequilibrium trend, as they undergo a gradual degradation due to chemical (i.e., corrosion) and biological (e.g., wood-boring organisms) formation processes (Foecke et al., 2010; Gregory, 2020; Pournou, 2017; Taormina et al., 2020). Nevertheless, sites in highly dynamic environments, leading to frequent changes in equilibrium states, are prone to accelerated disintegration (Quinn & Boland, 2010). Therefore, the state of a shipwreck site as a system, and its susceptibility to disruption, should always be assessed before implementing any in situ preservation measures (Astley, 2016).

The dynamism of underwater sites is often controlled by their hydrodynamic environment and sediment budget, defined as the rate of net supply or removal of different sediments to the wreck area (I. A. K. Ward et al., 1999). One of the key processes controlling the sediment budget and determining the integrity of underwater structures is seabed scour, which occurs as a result of magnified flow velocity around objects disrupting natural near-seabed currents (Quinn, 2006; Sumer & Fredsøe, 2002). In engineering applications, erosive scour processes are considered detrimental to the stability of underwater structures such as bridges and wind farm piles, which often require special mitigation measures. For example, in the Irish Sea, significant scour developed at the base of monopiles shortly after the construction of the Arklow Bank wind park, resulting in the need to use rock armour to mitigate further scouring (Whitehouse et al., 2011). Therefore, much attention has focused on geotechnical assessments of scour and related processes for offshore engineering purposes (e.g., Matutano et al., 2013; Melling, 2015; Sumer, 2007; Whitehouse et al., 2011).

Although scouring has been researched at shipwreck sites, studies have mostly focused on single surveys, investigating intricate depositional and erosional signatures, referred to as wreck marks (Caston, 1979; Garlan et al., 2015). To fully understand the dynamics of scour development, however, high-resolution bathymetric surveys should be conducted at least two times. This approach, referred to as "time-lapse" or "repeat surveying," has not been used very often to date (e.g., Astley, 2016; Bates et al., 2011; Brennan et al., 2016; Quinn & Boland, 2010; Stieglitz & Waterson, 2013), considering that 3 million shipwrecks are estimated worldwide (Croome, 1999; UNESCO, 2017).

As changes in sediment budget due to scour can ultimately lead to the exposure or burial of shipwrecks, it therefore, also controls oxygen availability, biological encrustation, corrosion rates, and pressure gradients exerted on hulls (Quinn, 2006; I. A. K. Ward et al., 1999), mechanisms significantly influencing site formation. The presence or absence of ongoing scour processes may also indicate whether a shipwreck site is in a stable or dynamic equilibrium. Considering all these points, it is critical that seabed change at shipwreck sites is understood at various time scales to fully assess their preservation potential.

The aim of this study is to expand the knowledge of formation processes at underwater shipwreck sites in the context of the sediment budget and the hydrodynamic environment. We achieve this by comparing the spatial and temporal development of scour signatures and other bedforms around 10 metal-hulled shipwrecks lost between 1875 and 1918, located at moderate depths (26–84 m) in contrasting hydrodynamic and sedimentary settings in the Irish Sea. Very high-resolution time-lapse bathymetric data were collected and integrated with seismics, sediment samples, and modeled near-seabed tidal currents. Bathymetric survey design was optimized to collect the highest resolution data possible, resulting in difference models and analysis of geomorphic change at a resolution previously unrealized in time-lapse assessments of underwater cultural heritage. The number of wrecks investigated and the combination of methods

provide new knowledge that allows for the development of more accurate underwater site formation models. In addition, we recognize this investigation as relevant for offshore engineering applications, as it focuses on localized morphodynamic change around submerged man-made structures.

2 | MATERIALS AND METHODS

2.1 | Study area

The study area encompasses the waters off the east and northeast coast of the island of Ireland from Rathlin Island in the north to Dublin Bay in the south (Figure 1). Within this area, 10 wrecks were investigated: *SS Lugano*, *SS Santa Maria*, *SS Tiberia*, *SS Chirripo*, *SS Polwell*, *FV St. Michan*, *SS WM Barkley*, *SS Hare*, *RMS Leinster*, and *HMS Vanguard*. With the exception of *HMS Vanguard*, all shipwrecks investigated in this study were lost due to naval warfare during World War 1. *HMS Vanguard* sank in fog in 1875 due to a collision with its sister ship *HMS Iron Duke*. The 10 shipwreck sites were selected to represent a range of physical environments, characterized by different tidal conditions and varied geological substrates. These shipwrecks are just a few of more than 18,000 other wrecking incidents that are recorded off the island of Ireland (Brady et al., 2012; Forsythe et al., 2000).

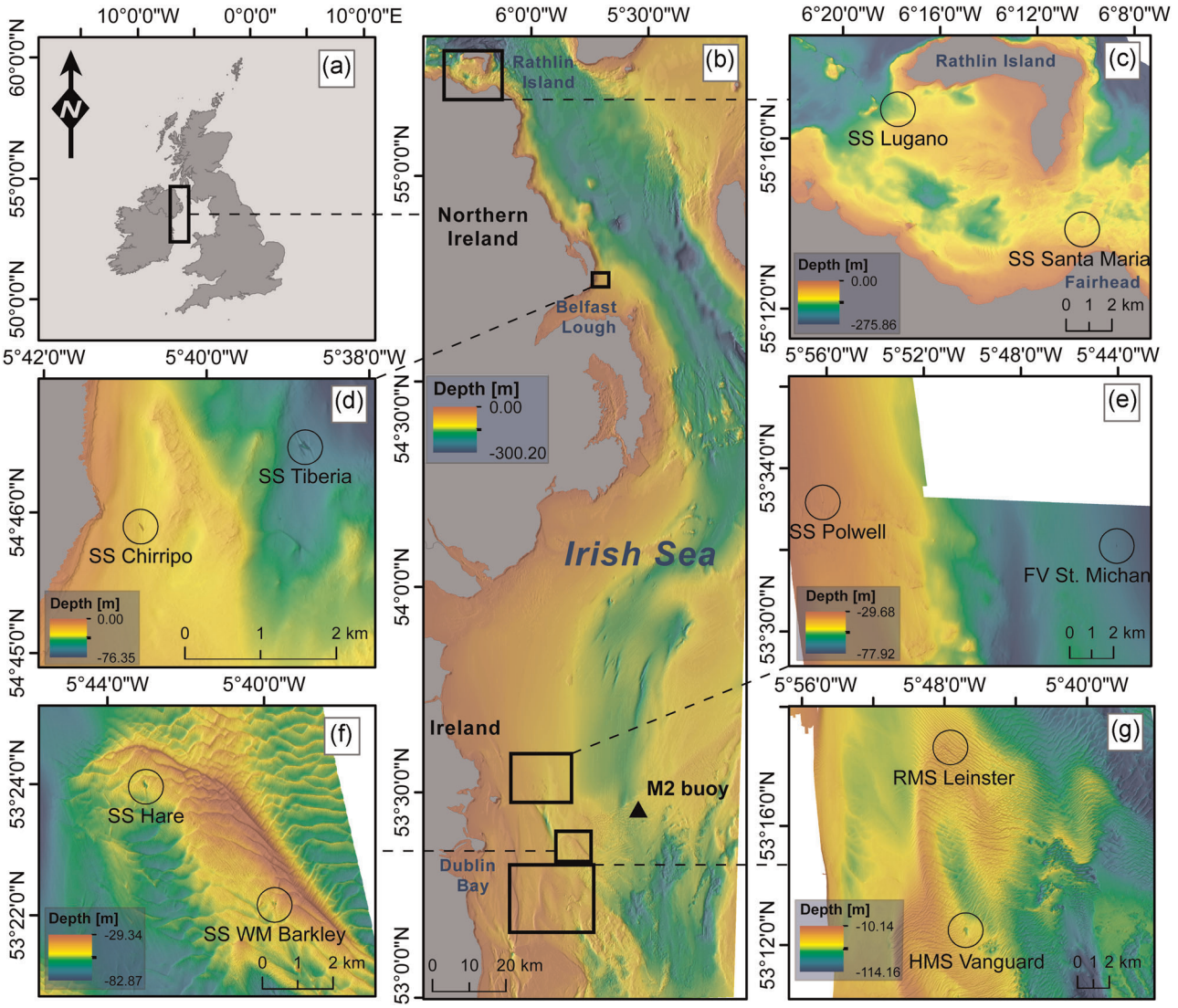

FIGURE 1 (a) Location of the study area on the map of the United Kingdom and Ireland. (b) Locations of the study sites in the Irish Sea with inset maps representing sites (c) between Fairhead and Rathlin Island, (d) off Belfast Lough, (e) northeast of Dublin, (f) east of Dublin, (g) southeast of Dublin. Backdrop bathymetry presented in Figure 1 was obtained from (b) EMODnet Bathymetry Consortium (2018), (c) Joint Irish Bathymetric Survey project (https://www.infomar.ie/partnerships/jibs-joint-irish-bathymetricsurvey), (d) Royal Navy (public sector information, licensed under the Open Government License v2.0), and (e–g) INFOMAR project [Color figure can be viewed at wileyonlinelibrary.com]

2.1.1 | Hydrodynamic regime

The Irish Sea is a shelf sea dominated by tidal currents that are typically rectilinear along coasts and in straits (Ozer et al., 2015). Semidiurnal lunar (M2) and solar (S2) tides propagating from the Atlantic Ocean through the North Channel to the north and St. George's Channel to the south largely control the tidal current magnitudes (Neill et al., 2014; Ozer et al., 2015). The areas chosen for the study (Figure 1) are characterized by depth-averaged peak spring tide magnitudes ranging from 0.5 m/s around Belfast Lough (Atkins, 1997), 1 m/s off Dublin Bay (Howarth, 2001), to 3 m/s in Rathlin Sound. The latter is a candidate area for tidal turbine development (Lewis et al., 2015; Pérez-Ortiz et al., 2017), whereas offshore Dublin Bay is proposed for offshore wind development.

Flows in the Irish Sea are also influenced by surface waves, inertial currents, residual currents, and storm surges. Waves are generally characterized by a short period with a limited access of swell waves to the basin, as it is partly enclosed. In general, tidal current amplitudes are an order of magnitude greater than long-term averaged residual currents (Bowden, 1980). Inertial currents, episodically generated in the thermally stratified waters of the western Irish Sea, are observed to reach 0.2 m/s in the surface layer (Sherwin, 1987). The circulation in this part of the basin is also affected by a density-driven cyclonic gyre that forms during spring and summer, with modeled baroclinic currents reaching 0.14 m/s (Horsburgh & Hill, 2003). The largest nontidal, depth-averaged current magnitude has been reported to reach 0.65 m/s in the North Channel (east from Belfast Lough; Figure 1), which was attributed to a storm event (Knight & Howarth, 1999). Externally generated storm surges propagating from south and north appear to interact with tides causing twice-daily intermittent oscillations (Howarth, 2001). Nevertheless, the prevailing flows in the whole basin remain tidally generated.

2.1.2 | Geological setting

The Irish Sea was glaciated during the Last Glacial Maximum (27 ka–18 ka BP; Scourse et al., 2019; Van Landeghem & Chiverrell, 2020) when the Irish Sea Ice Stream advanced through the Irish Sea, eroding and reworking sediment, and depositing variable thicknesses of glacial diamict. This diamict was often deposited directly on the bedrock and is referred to as the upper till member (Jackson et al., 1995). The upper till member comprises sand to boulder-grade material and is often overconsolidated (Coughlan et al., 2019; Mellet et al., 2015). During the retreat phase of the Irish Sea Ice Stream during deglaciation, large amounts of meltwater were discharged along with outwash material in the form of a heterogeneous mix of sediments, predominately gravels, with mud, sand, and cobbles, referred to as the chaotic facies (Coughlan et al., 2019; Jackson et al., 1995).

The subsequent marine transgression and present-day hydrodynamics reworked much of the glacial and postglacial sediment in the south Irish Sea into a mosaic of substrates (S. L. Ward et al., 2015). These processes created a series of dynamic bedforms, including migrating sediment waves, in an area dominated by coarse lag deposits. The sediment waves vary in size and morphology, with the magnitude of migration highest in the central Irish Sea, with average rates of up to 35 m/year, decreasing northward (Van Landeghem, Uehara et al., 2009; Van Landeghem et al., 2012; Coughlan et al., 2020). The northward transport of sediment eventually terminates in an area of low bed stress, referred to as the Western Irish Sea Mud Belt, where the fine-grained sediment has been accumulating since the end of the last glaciation (Belderson, 1964; Woods et al., 2019). In this area, there are thick deposits (up to 40 m) of stratified gray-brown muddy sands with silts and clays referred to as the mud facies (Jackson et al., 1995). This mud facies is typically of low shear strength and so potentially prone to scour around obstacles (Coughlan et al., 2019).

2.2 | Data acquisition and processing

2.2.1 | Time-lapse MBES data

Time-lapse surveys were designed to provide high-resolution MBES coverage for the selected shipwreck sites in 2015, 2016, and 2019 (Table 1). The 2015 and 2016 data comprise single surveys for selected wrecks, whereas in 2019, repeat surveys spaced 1 week apart were also conducted for three sites. The first survey took place before a spring tide (October 28, 2019) and stormy weather (October 29, 2019–November 3, 2019; Table 1, referred to as 2019a), after which the second, repeat survey was conducted (Table 1, referred to as 2019b). Additional lower resolution MBES legacy data from 2010 were included in the research to provide multiannual (2019–2010) change comparisons for the *SS Hare* and *SS WM Barkley* sites (Table 1). All the data were collected on the Marine Institute's *RV Celtic Voyager* during Integrated Mapping for the Sustainable

TABLE 1 Multibeam echosounder time-lapse survey data availability for the candidate shipwrecks

Shipwreck	2010	2015	2016	2019a	2019b
SS Lugano			✓		
SS Santa Maria			✓		
SS Chirripo		✓	✓		
SS Polwell		✓	✓	✓	✓
SS Tiberia		✓	✓		
FV St Michan		✓		✓	
RMS Leinster		✓	✓	✓	
HMS Vanguard		✓			✓
SS Hare	✓	✓	✓	✓	✓
SS WM Barkley	✓	✓	✓	✓	✓

Note: 2019a and 2019b correspond to surveys before and after a storm/spring tide, respectively.

Development of Ireland's Marine Resource (INFOMAR) project's survey CV10_01 and ship-time application surveys CV15021, CV16031, CV19027.

The 2015, 2016, and 2019 surveys were designed specially to capture the shipwreck site and surrounding seabed including the full extent of observed wreck marks at a high spatial resolution. The same line plan was used through these surveys with slight ad hoc changes in line orientations due to weather constraints and to improve survey efficiency. Infill profiles were acquired in places where the vessel deviated from lines, to avoid creating holes in the data sets. Survey grids were planned to ensure 100% overlap, thus achieving 200% coverage. The vessel was moving between 3 and 5 knots during all surveys. This strategy ensured consistency between the acquired data sets and allowed imaging of the site's local geomorphology at the highest possible resolution.

The 2015 MBES data were acquired between 5 and 11 September using a hull-mounted single-head Kongsberg EM2040 operating at 400 kHz, a continuous wave (CW) pulse, and 110°–120° swath coverage. Integrated GNSS/L-Band receiver CNAV 3050 was used for primary position corrections with a Seatex Seapath 330+ acting as a secondary positioning system and providing motion referencing and timing. Sound velocity profiles for refraction corrections were acquired with a Valeport Midas SVP and real-time AML surface sensor. The October 4–10, 2016 and October 24–November 5, 2019 survey data were collected using the same survey setup, but with a dual-head Kongsberg EM2040 MBES.

The legacy MBES data were collected in May 2010 using a hull-mounted single-head Simrad EM3002 operating at 300 kHz and a short CW pulse with a 100° swath angular coverage. Positional information was supplied by a combination of Seatex Seapath 200 DGPS and Fugro HP DGPS. Several onshore and offshore tide gauges were deployed to provide tidal corrections. The tidal data were later leveled to a chart datum using Vertical Offshore Reference Frames. The 2010 data were collected using a different survey design, which followed the Maritime and Coastguard Agency (MCA) guidelines for wreck surveys (MCA, 2016), optimizing detailed wreck coverage over seabed contextualization.

All MBES bathymetric data were cleaned with the Combined Uncertainty and Bathymetry Estimator algorithm (CUBE; Calder & Wells, 2006), and corrected for tides and refraction using CARIS Hips and Sips v. 9.1 software. The processed data were exported to rasterized digital elevation models (DEMs) in the UTM 30N projection. Quality control was performed using crosslines, which indicated at least 98% compliance with IHO Special Order standard (IHO, 2020). The 2015, 2016, and 2019 bathymetric data sets were gridded to a common 30-cm spatial resolution for the time-lapse analysis. The 2010 data were gridded to the best achievable 50-cm resolution; thus, for the *SS Hare* and *SS WM Barkley* sites, the 2015 and 2019 data were additionally gridded to this resolution to ensure the same resolution for multiannual data comparisons (Table 1).

2.2.2 | Seismic data

Shallow seismic data were collected for the *HMS Vanguard* site during the 2015 MBES survey, using an SES probe 5000 sub-bottom profiler operating at 3.5 kHz. Raw data were exported from CODA Octopus v. 7.3.3 after applying a bandpass filter. Manual horizon picking was then performed in Adobe Illustrator 2020 to inform vertical constraints for scour development at the site.

2.2.3 | Sediment samples

Sediment samples were collected using a Shipek grab inside and outside the erosional and depositional signatures. The granulometric analysis of the sediments was performed using a MALVERN Mastersizer 3000 laser diffraction particle size analyzer for fractions with grain sizes <2.38 mm, with an exception for the samples collected at the *FV St. Michan* and *HMS Vanguard* sites, which were analyzed using a sieve stack. Sediment classification into Folk classes (Folk, 1954) and median grain size (d_{50}) calculations including >2.38 mm particle sizes (i.e., gravel) were performed using Gradistat v. 8 software (Blott & Pye, 2001). In cases where samples indicated gravelly components in the mixture or gravel as a main fraction, a nominal value of 4 mm was used to represent gravel in the median grain size calculations.

2.2.4 | Oceanographic data

Current velocity magnitudes and directions at 1 m above the seabed were obtained for the wreck sites from an operational model run by the Marine Institute of Ireland (Nagy et al., 2020). The model is an implementation of the Regional Oceanic Modeling System (ROMS; Shchepetkin & McWilliams, 2005) for an area of the northeast Atlantic encompassing all Irish waters. The horizontal resolution of the model in the Irish Sea is between 1.1 and 1.7 km, and the temporal resolution of the model data is hourly. Models for *SS Santa Maria* and *SS Lugano* cover 1-year period (January 31, 2019–December 31, 2019), and those for all other sites cover two years (January 01, 2017–December 31, 2019).

Significant wave height and wave period data were obtained from an Ocean Data Acquisition Systems (ODAS) M2 buoy located around 20 nm east of Dublin (53°28′8″N 5°25′5″W, 95-m water depth; Figure 1b), which is a part of the Irish Marine Data Buoy Observation Network managed by the Marine Institute (Ireland) in collaboration with Met Éireann and the UK Met Office. The data cover a time period from May 03, 2001 to April 22, 2020, with some gaps.

2.3 | Data analysis

The first step of the analysis procedure was to thoroughly characterize each site using the MBES and ROMS data. This entailed determining dimensions and depths of the shipwrecks and associated erosional/depositional signatures, their orientation relative to dominant tidal currents, and calculating the volume of eroded/deposited sediment. The second step was to determine sediment mobility from the collected sediment samples and ROMS data. This

entailed calculating sediment mobility thresholds and the frequency of threshold exceedance for each site. The third step was to detect and quantify geomorphic change within the intervals covered by time-lapse bathymetric surveys. This included calculation of volumetric changes in sediment budget and maximum scour depths at each site. Effectively, this sequence enables us to characterize in detail the baseline oceanographic, bathymetric, and sedimentological conditions at each site (Steps 1 and 2) and, with this in hand, explore and advance secure explanations for the patterns of geomorphic change identified in Step 3. The procedure followed in each step is explained below.

2.3.1 | Site characterization

Data integration and analysis were conducted using ESRI ArcMap v. 10.6.1 GIS software. The DEMs were analyzed to measure the dimensions and orientations of the shipwrecks. Initial volumes of shipwreck-induced erosional and depositional signatures were calculated for the oldest time-step DEMs with extents covering the whole signatures. The 2015 DEMs were used for the calculation of initial volumes and maximum scour depths for every shipwreck, except for *SS Lugano* and *SS Santa Maria*, for which the 2016 DEMs were used. To perform the volume calculations, the extents of the wreck marks were delineated. As manual delineation through vectorization is highly subjective, the residual relief modeling approach of Majcher et al. (2020) was used to separate the wreck marks from the surrounding geomorphology. The methodology relies on a high-pass filtered DEM (Majcher et al., 2020; Walbridge et al., 2018; Wessel, 1998), combined with a breakpoint classifier. Separate high-pass filtered moving mean kernels were chosen to delineate erosional and depositional signatures. High-pass filtered DEMs were then masked using the extents of the erosional scour features delineated by the breakpoint classifier. The 3D Analyst surface volume tool was used on these masked high-pass filtered DEMs to calculate volumes of all the pixels with values below (erosion) and above (deposition) zero. Shipwreck structures were removed for the volumetric calculations using clipping and masking tools.

2.3.2 | Sediment mobility

Current velocities derived from the ROMS model and sediment samples were used to estimate how often sediment may be mobilized at the candidate sites, according to the approach prescribed by Whitehouse (1998) and Soulsby (1997). In this method, the potential mobility of sediment can be assessed by comparing the values for current-related bed shear stress (τ_c) with the critical shear stress (τ_{cr}) and calculating exceedance levels ($\tau_{cr} < \tau_c$). The current-related bed shear stress is calculated using the following equation:

$$\tau_c = \rho C_D \bar{U}^2, \quad (1)$$

where ρ is the water density, C_D the drag coefficient, and $\bar{U}$ the depth-averaged current speed. The critical shear stress is then defined by the following:

$$\tau_{cr} = \theta_{cr} \times g\,(\rho_s - \rho)\,d_{50}, \quad (2)$$

where θ_{cr} is the critical Shields parameter, g is the acceleration due to gravity (9.81 m/s^2), ρ_s (1700 kg/m^3; Tenzer and Gladkikh, 2014) and ρ (1027 kg/m^3) are densities of sediment and water, respectively, and d_{50} is the median grain size.

The presence of an obstacle to a flow causes its contraction and increase in speed, hence, increasing shear stresses exerted on the bed downstream of the obstacle (Soulsby, 1997; Whitehouse, 1998). Therefore, in this study, exceedance levels were calculated separately, assuming a fourfold shear stress amplification factor determined by Smyth and Quinn (2014) through computational fluid dynamic simulations, conducted using a 3D model of a shipwreck derived from high-resolution MBES data in the Irish Sea. The calculations of the exceedance levels presented in the results were averaged for each studied shipwreck site. Shear stress calculations for all the sediment samples are included as Supporting Information.

Furthermore, to assess the influence of waves at the sites, the 99th percentile representing storm events (Matulla et al., 2008; Wang & Swail, 2001) was calculated for 122,222 buoy readings of significant wave heights. According to an approximation by Soulsby (1997), oscillatory flows induced by waves can affect the seabed when the following relation is satisfied:

$$h < 10H_s, \quad (3)$$

where H_s is significant wave height and h is water depth at the seabed. The calculated 99th percentile of the distribution of significant wave heights (H_{s99}) recorded at the M2 buoy was, therefore, used with Equation (3) to assess the wave influence on the sediment mobility at the sites. The wave data were analyzed separately for the period of the 2019 survey (between October 24 and September 5, 2019) to assess the wave regime for the weekly time-lapse bathymetric coverage.

2.3.3 | Bathymetric time-lapse analysis

The time-lapse analysis of the bathymetric data sets comprised multiple steps. First, DEMs of Difference (DoD) were obtained by a subtraction of DEMs corresponding to subsequent surveys, using a raster minus tool. Shipwreck structures were masked in the DoDs, as they introduce outliers in bathymetric time-lapse analyses (Astley, 2016). Additionally, the study concentrates on geomorphic change at the sites and not on structural changes of the shipwrecks themselves. Recording the latter would require a different approach to survey design (e.g., Westley et al., 2019) and data analysis involving comparisons of dense point clouds rather than the DEMs.

Measured depth uncertainties were approximated for each bathymetric DEM using vertical total propagated uncertainty values

(vTPU) calculated by the CUBE algorithm during the multibeam data processing. These vTPU values, corresponding to any two compared DEMs, were combined using Equation (4), which provides a combined minimum level of detection threshold (LoD_{min}; Brasington et al., 2003):

$$LoD_{min} = \sqrt{(vTPU_{survey1})^2 + (vTPU_{survey2})^2}. \quad (4)$$

All recorded geomorphic changes contained within the minimum level of detection are considered unreliable. The vTPU values determined for the 2015, 2016, and 2019 surfaces are equal to 20 cm; therefore, the LoD_{min} value of the resulting DoDs is approximately ±30 cm. The vTPU values for the 2010 surfaces were not possible to estimate absolutely, but an examination of the acquired MBES data and analysis of equipment errors indicated that the same LoD_{min} values can be applied. Therefore, volumetric change calculations did not include pixel values within the LoD_{min} range (±30 cm).

After obtaining the DoDs, volumetric changes were calculated within 50-, 100-, 200-, 300-, 400-, and 500-m radii from the central positions of the shipwrecks, depending on the maximum extent of the DoD rasters. These radii were inspired by buffers that have been applied to UK historic shipwrecks in the eastern Irish Sea, designated under the Protection of Wrecks Act (1973) and which range between 100 and 500 m (Wessex Archaeology, 2005). The smallest (50 m) radius was chosen to investigate changes in the immediate vicinity of the shipwrecks.

Lastly, the time-lapse analysis involved a comparison of maximum scour erosion depths for all the time steps in relation to the depth of the surrounding seabed. As the seabed outside of the scour-impacted areas may be mobile, the surrounding seabed depths were picked in the oldest time-step DEMs and used for all subsequent time steps.

3 | RESULTS

3.1 | Site characterization

In this section, the results of the analysis of the bathymetric DEMs, modeled near-seabed current data, and sediment samples are presented. The granulometric analysis of the sediment samples collected around the wrecks resulted in a classification of the sites into three categories: sand-dominated, multimodal, and gravel-dominated sites.

3.1.1 | Sand-dominated sites

RMS Leinster, *HMS Vanguard*, *SS Hare*, and *SS WM Barkley* rest on largely sandy substrates (Figure 2 and Table 2) and are surrounded by bifurcating sediment waves superimposed on larger sediment waves (Stow et al., 2009; Van Landeghem, Wheeler et al., 2009). Modeled near-seabed current directional distributions vary slightly across these sites (Figure 2), with maximum spring tide magnitudes oscillating around 0.5 m/s (Table 2).

RMS Leinster has an erosional depression with a maximum depth of 3.00 m on its SE side and a depositional tail extending south from the wreck (Figure 2a). Both of these sedimentary signatures are aligned with the most frequently modeled near-seabed current oriented N–S. The erosional signature merges with a natural depression, which may be a result of shipwreck- or sediment wave-induced scour, and is aligned to the less frequent NNW–SSE currents. The wreck is bounded to the south and north by separate, large sediment waves characterized by a height of 5–8 m and a wavelength of 200 m. Ubiquitous bifurcating sediment waves, with heights and wavelengths typically not exceeding 0.5 and 15 m, respectively, are imaged around the wreck, including outside and inside the erosional and depositional zones. They are mostly perpendicular to the currents oriented NNW–SSE. However, the large sediment waves are not aligned with any component of the modeled currents, being oriented NNE–SSW. The total volumes of erosion and deposition are low at this site in comparison to other wreck sites located in the same sand substrate (Table 2).

SS Hare and *SS WM Barkley* are located within 5 km of one another in the same sediment wave field (see Figure 1f). Both wreck sites are characterized by deep scour pits extending from their bow and stern (Figures 2b and 2c). *SS Hare*'s pits have a maximum depth of 11.32 m in relation to the surrounding seabed and stretch up to 200 m from the wreck (NW direction; Table 2). *SS WM Barkley's* pits have a similar geometry, reaching a distance of 285 m from the shipwreck, with a maximum depth of 13.64 m. In both cases, the scour pits are separated by thin depositional ridges, parallel to the weaker, less frequent currents oriented N–S, whereas the scour pits correspond to the stronger NNW–SSE currents. Pervasive sediment waves, with typical wavelengths of 10–15 m and height up to 0.5 m, are developed at both sites, aligned with modeled current directions, and are present inside the scour pits. Large sediment waves, 7- and 4-m high for *SS Hare* and *SS WM Barkley*, respectively, are present at the north of the sites. Their wavelengths are difficult to determine, as the large sediment wave field is highly irregular. Multiple grab samples collected at the *SS Hare* site indicate the presence of sand and gravelly sand inside the pits (Table 2). High volumes of sediment are eroded at these sites, among the highest of all the candidate shipwreck sites (Table 2).

At the *HMS Vanguard* site, an 11.69-m deep comet scour has developed, aligned with the bidirectional current regime (Figure 2d), reaching as far as 280 m south of the shipwreck. The shipwreck itself is entrenched between two depositional features, much smaller in size and volume (Table 2). Scour development is constrained by a large sediment wave to the NE of the site. The change in bathymetry from the base of the scour pit to the large sediment wave's crest reaches up to 13 m. Smaller sediment waves, typically 10–15 m in length and 0.2–0.5 m in height, are present around the site, perpendicular to the currents; however, they are not developed in the central part of the scour pit. Three unsuccessful attempts to collect grabs from the scour pit indicate a coarser/hard substrate. Corroborating evidence comes from the seismic data acquired over the site, where laterally continuous,

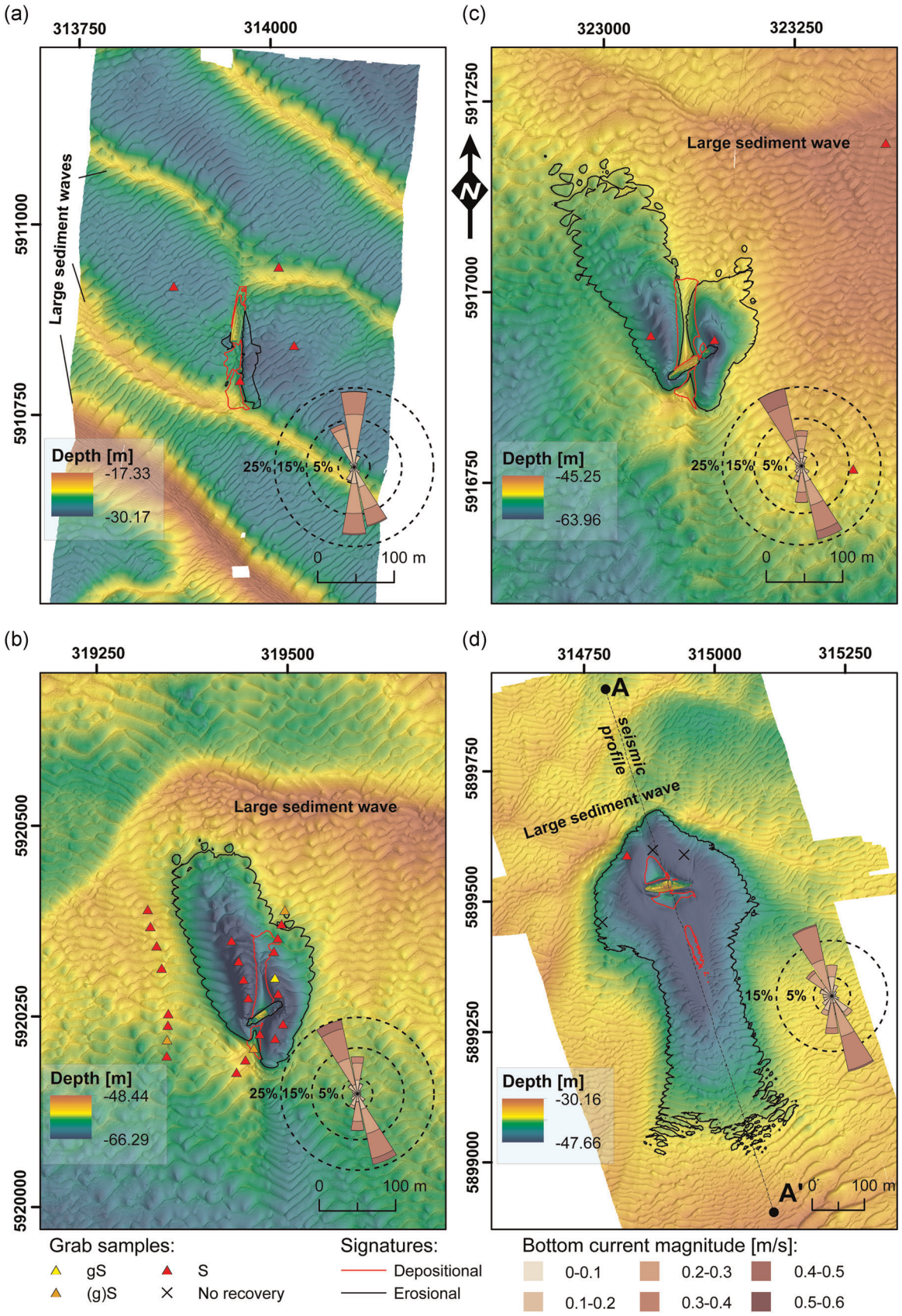

FIGURE 2 Sand-dominated sites presented as digital elevation models with a multidirectional hillshade occlusion: (a) *RMS Leinster*, (b) *SS WM Barkley*, (c) *SS Hare*, (d) *HMS Vanguard* (the seismic profile is described in Figure 3). Rose charts represent the modeled near-seabed current data. Grab samples: gS, gravelly sand; (g)S, slightly gravelly sand; S, sand [Color figure can be viewed at wileyonlinelibrary.com]

TABLE 2 Characterization of the shipwreck sites

Category	Wreck	Length, width, height (m)	Seabed depth (m)	Year of loss	Orientation	Peak seabed current (m/s)	Maximum reach of signatures from a wreck		Sediment—Folk (1954) classification			Initial volumes (m^3)		$\tau_{cr} < \tau_c$ (%) threshold exceeded	$\tau_{cr} < \tau_c$ (%) amplified
							Erosional (m)	Deposi-tional (m)	Signatures–ero-sional	Signatures–depositional	Outside signatures	Erosion	Deposition		
Sand	*RMS Leinster*	110 × 13 × 5	28	1918	188°, aligned/ oblique to currents	0.45	90	50	No data	Sand	Sand	1635	1213	43.9	79.0
	SS Hare	53 × 9 × 7	61	1917	55°, nearly perpendicular to currents	0.51	200	92	Sand/ gravelly sand	Sand/ gravelly sand	Sand	121,235	3264	52.7	85.5
	SS WM Barkley	72 × 10 × 5	52	1917	54°, nearly perpendicular to currents	0.54	285	107	Sand	No data	Sand	108,187	6211	56.1	87.6
	HMS Vanguard	90 × 20 × 12	40	1875	82°, perpendicular to currents	0.47	280	120	No recovery/ sand	No data	No data	345,385	3897	56.6	91.2
Multimodal	*SS Chirripo*	115 × 15 × 12	26	1917	146°, oblique to currents	0.28	–	700	No scour recorded	Gravelly muddy sand	More gravel/ muddy sandy gravel	–	415	2.3	52.5
	SS Tiberia	127 × 17 × 10	55	1918	285°, oblique to currents	0.53	110	500	Muddy sandy gravel	Slightly gravelly muddy sand	Muddy sand	17,631	18,296	50.6	79.1
	SS Polwell	95 × 12 × 10	26	1918	208°, oblique to currents	0.38	1290	1190	Gravelly muddy sand	Muddy sand	Muddy Sand	19,286	14,047	17.2	69.5
	FV St. Michan	30 × 6 × 5	72	1918	104°, perpendicular to currents	0.35	100	–	No recovery/ muddy sandy gravel	Muddy sand/grav. mud/grav. and slightly grav. muddy sand	Mud	8526	3038	32.5	70.8
Gravel	*SS Lugano*	106 × 16 × 10	84	1917	97°, aligned with currents	0.82	–	120	No scour recorded	No data	Sandy gravel/ gravel	–	114	4.9	58.5
	SS Santa Maria	100 × 16 × 16	67	1918	104° (hull), oblique to currents	0.97	140	–	Gravel/boulders	No deposition recorded	Gravel/boulders	21,463	–	19.0	67.4

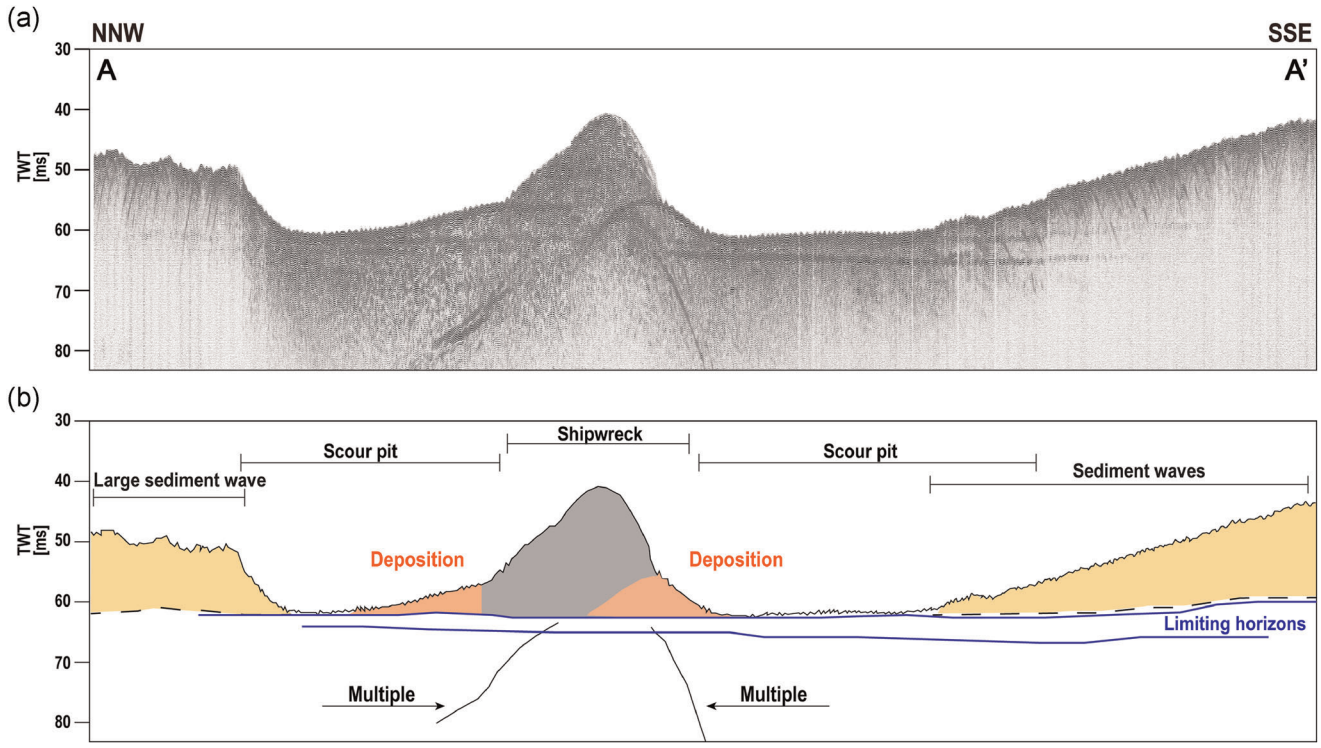

FIGURE 3 (a) Seismic line acquired over *HMS Vanguard* and (b) its interpretation, showing the digitized horizons vertically limiting further development of the scour pits. The profile's location is shown in Figure 2d. Sediment waves and a large sediment wave are visible SSE and NNW of the wreck, correspondingly. Multiple reflections (seismic artifacts) are marked separately [Color figure can be viewed at wileyonlinelibrary.com]

shallow medium amplitude horizontal reflectors at 0–10 m below the seafloor (Figure 3) are interpreted as hard layers, acting as a vertical constraint for scour development. The *HMS Vanguard* site is also characterized by the highest volume of erosion among all the recorded sites (Table 2).

3.1.2 | Multimodal sites

SS Chirripo, *SS Tiberia*, *SS Polwell*, and *FV St. Michan* rest on mixed substrates (Table 2), characterized by a multimodal distribution of sediment fractions. The modeled current magnitudes vary across sites, with the weakest currents not exceeding 0.3 m/s at *SS Chirripo*, reaching 0.4 m/s for *SS Polwell* and *FV St. Michan*, and exceeding 0.5 m/s for *SS Tiberia* (Table 2).

At the *SS Chirripo* site, distinctive thin (width: 10–15 m), typically 0.2–0.4 m high, elongate depositional signatures extend symmetrically up to 700 m from the shipwreck (Figure 4a). A slight offset between the directions of these features and the modeled current directions is noted. A group of pockmark-like holes is imaged W, NW, and N of the shipwreck (Figure 4a). They are circular, with approximate radii of 15 m and depths of 0.4–1 m. The granulometric analysis of the sediment samples indicates gravelly muddy sand on the depositional wreck marks, whereas gravel becomes more dominant away from these. No distinct scour zone is recorded at this site.

SS Tiberia, located 2.4 km NE of *SS Chirripo*, exhibits an intricate pattern of nearly symmetrical depositional and erosional signatures, aligned with the modeled currents (Figure 4b) and reaching up to 500 m from the shipwreck (in NW direction). Two scour pits with maximum depths of 4.27 m are formed in immediate proximity to the wreck, extending from the bow and stern. The depositional ridges and erosional troughs extend far from the wreck (Figure 4b), with variable lengths and widths. Sediment samples show muddy sandy gravel inside the scour pits and slightly gravelly muddy sand on the depositional signatures, whereas the seabed outside of the wreck marks comprises muddy sand (Table 2). In terms of sediment volumes, the erosional and depositional zones are of similar magnitude (Table 2).

The longest flow-aligned depositional and erosional signatures are developed at the *SS Polwell* site, where ridges extend for 1190 m and scour features for 1290 m, respectively, parallel to modeled NNW-orientated peak tidal flow (Figure 4c). The wreck marks, less developed in the SSE direction, also have up to 100-m width, with the deepest depression and the highest elevation in relation to the ambient seabed being 1.48 and 1.00 m, respectively. Gravelly muddy sand is recorded in the erosional signature stretching to the NNW, whereas the rest of the samples indicate muddy sand (Figure 4c). At this site, the volume of eroded material calculated from the relief modeling is slightly higher than for the deposited material (Table 2).

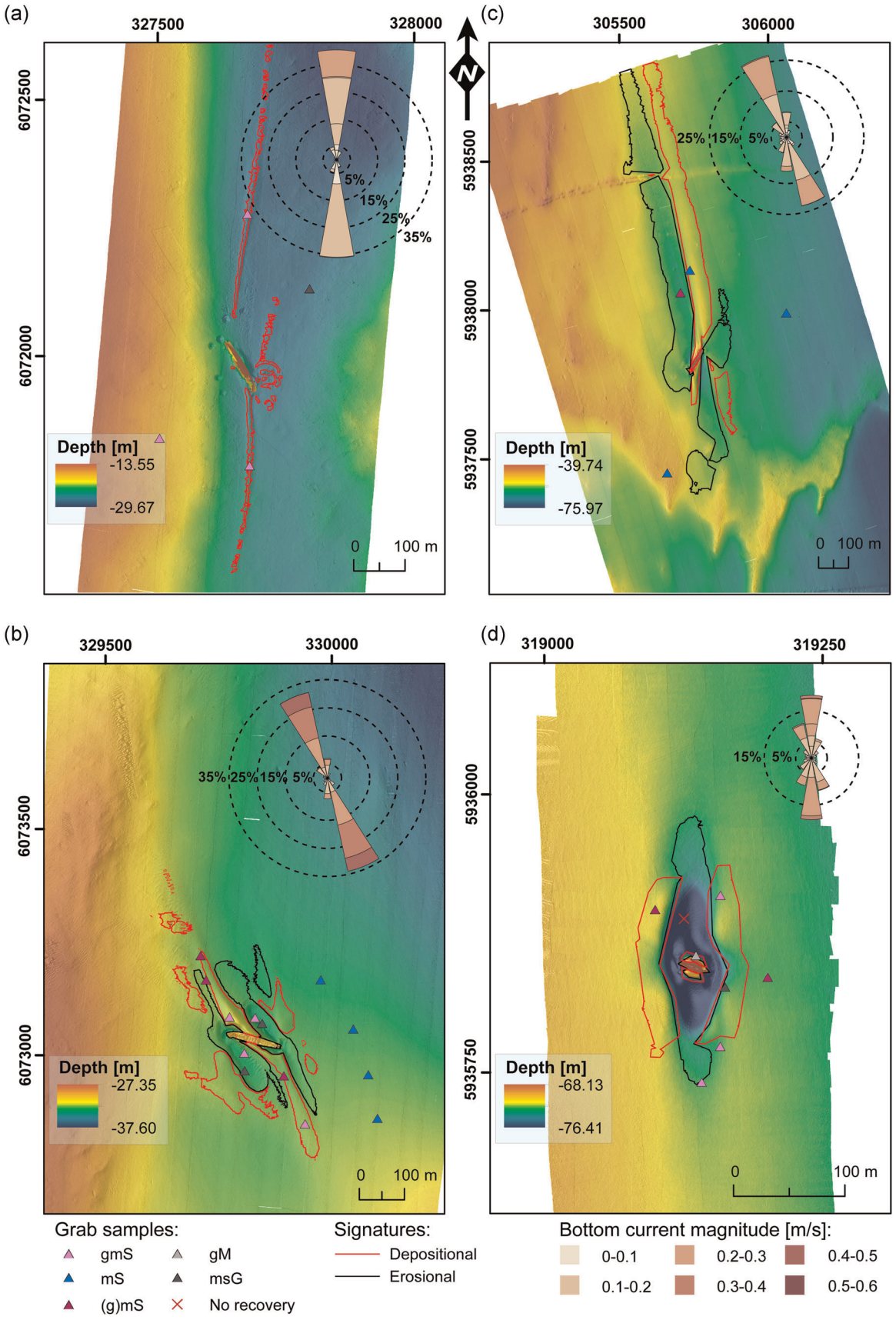

FIGURE 4 Multimodal sites presented as digital elevation models with a multidirectional hillshade occlusion: (a) *SS Chirripo*, (b) *SS Tiberia*, (c) *SS Polwell*, (d) *FV St. Michan*. Rose charts represent the modeled near-seabed current data. Grab samples: gM, gravelly mud; gmS, gravelly muddy sand; (g)mS, slightly gravelly muddy sand; mS, muddy sand; msG, muddy sandy gravel [Color figure can be viewed at wileyonlinelibrary.com]

FV St. Michan rests on the boundary of the Western Irish Sea Mud Belt, an area that typically experiences lower bed stresses than the surrounding sand-dominated areas (Belderson, 1964; Coughlan et al., 2020). Nevertheless, a deep scour pit has developed around the shipwreck with a maximum depth of 4.34 m (Figure 4d). The shipwreck, which is much smaller in comparison to the other investigated vessels (Table 2), is elevated above the pit on a sediment mound (Figure 4d). Some material has been redeposited around the pit, which is, therefore, reflected in the calculated depositional volume (Table 2). Sediment samples were highly multimodal. The muddy sandy gravel is recorded close to the boundary of the scour pit. Attempted sampling was unsuccessful inside the pit, indicating a coarse sediment. Gravelly mud is recorded in the depositional mound proximal to the shipwreck, and slightly gravelly and gravelly muddy sands are present in the depositional signatures outside the scour pit and in the surrounding seabed (Figure 4d).

3.1.3 | Gravel-dominated sites

SS Lugano and *SS Santa Maria* are located on coarser substrates as compared with the other sites, which is reflective of a much stronger tidal regime, with peak modeled flows of 1 m/s (Table 2). *SS Lugano* is situated on a sandy gravel and gravel bed, with a small depositional zone near the bow and lacking any erosional signature. A narrow (around 10-m width) low-profile (0.1–0.2 m) depositional braid extends 120 m SSE from the shipwreck, probably comprising a finer sediment (Figure 5a). In contrast, at the *SS Santa Maria* site located 9.6 km SE of *SS Lugano*, there exist significant flow-aligned erosional signatures (Table 2) with depths exceeding 5 m up to 140 m from the broken bow of *SS Santa Maria* (Figure 5b). At this site, no clear depositional zone is imaged.

3.2 | Sediment mobility

3.2.1 | Current-induced sediment mobility

Bed shear stresses modeled from current values for each wreck site were compared against granulometric data from sediment samples to calculate how often sediment mobilization thresholds were exceeded to determine the dynamism of these sites. Sand-dominated wreck sites generally exhibit high levels of sediment threshold exceedance values, with averages of 43.9%, 52.7%, and 56.1% for the

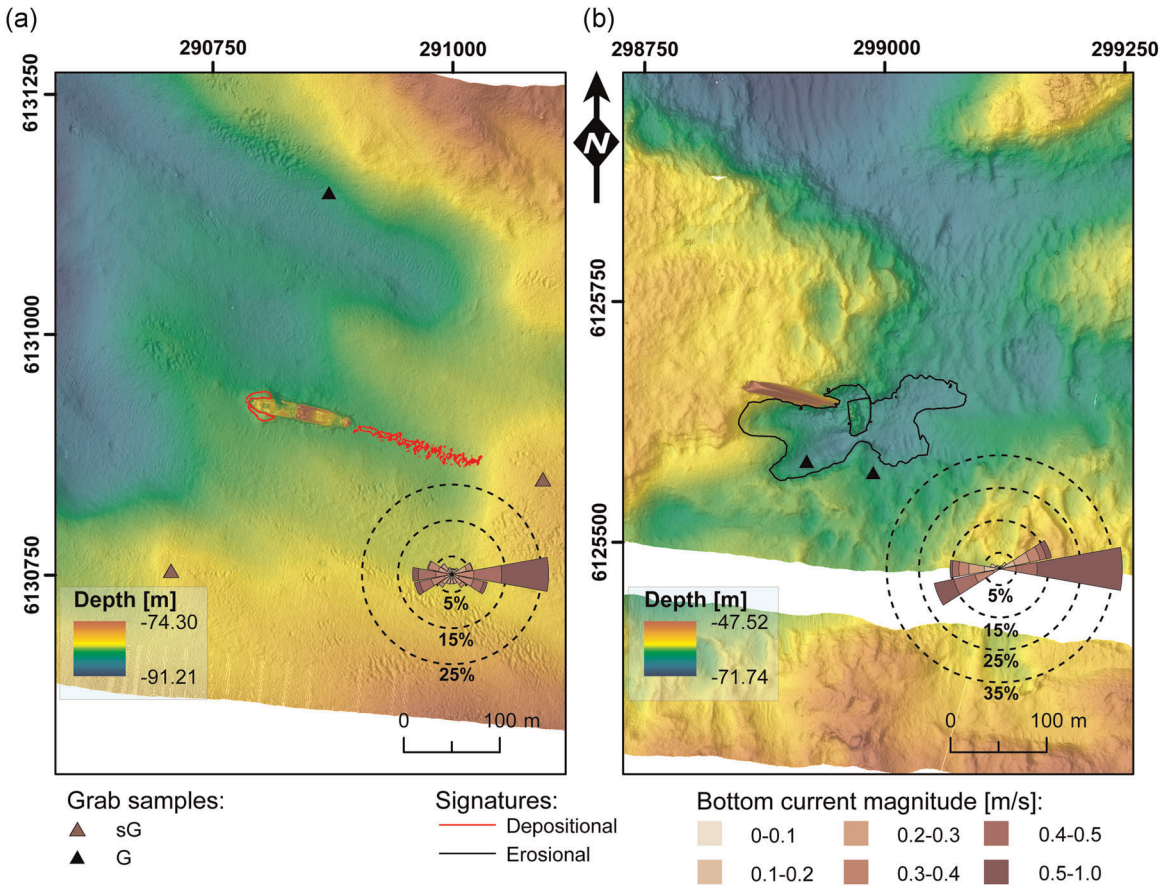

FIGURE 5 Gravel-dominated sites presented as digital elevation models with a multidirectional hillshade occlusion: (a) *SS Lugano*, (b) *SS Santa Maria*. Rose charts represent the modeled near-seabed current data. Grab samples: G, gravel; sG, sandy gravel [Color figure can be viewed at wileyonlinelibrary.com]

RMS Leinster, *SS Hare*, and *SS WM Barkley*, respectively (Table 2). Sediment threshold exceedance values for the multimodal sites exhibit the broadest range, most likely due to the geographic and regional differences between these sites. However, despite their relative proximity, the exceedance levels calculated for samples from the SS *Chirripo* site (2.3%) were significantly lower than those for the samples from *SS Tiberia* (50.5%). Exceedance levels for sample data at the *SS Polwell* are relatively low at 17.2%. Wrecks in gravel-dominated settings exhibit low exceedance values, 4.9% for the *SS Lugano* site and limited exceedance of 19% at the *SS Santa Maria* site (Table 2). When the fourfold shear stress amplification factor established by Smyth and Quinn (2014) is applied to these sites, exceedance levels were exceeded at least 50% of the time for all sites. Greatest exceedances are modeled for the *SS WM Barkley* and *HMS Vanguard* sites, 87.6% and 91.2% of the time, respectively.

3.2.2 | Wave influence

The analysis of the M2 wave buoy (Figure 1b) data shows that the calculated 99th percentile of significant wave height distribution is 3.5 m (18-year return period). According to Equation (1), only wreck sites shallower than 35 m are directly affected by storms in the study area. The *SS Chirripo*, *RMS Leinster*, and *SS Polwell* sites meet this criterion, but they are all located closer to the western shore of the Irish Sea than the M2 buoy, and hence, are assumed to be partly sheltered with a very limited wave influence. During a storm event that disrupted the 2019 survey, the significant wave height did not exceed 3 m; hence, none of the sites surveyed in the period were directly influenced by waves.

TABLE 3 Maximum depths and annual changes of bed erosion (relative to a preceding time step) due to scour at the sites

Category	Shipwreck	Year	Max. scour depth (m)	Change (m)
Sand	*RMS Leinster*	2015	−3.00	–
		2016	−2.99	+0.01
		2019	−3.00	–
	HMS Vanguard	2015	−11.69	–
		2019	−11.63	+0.06
	SS Hare	2010	−11.38	–
		2015	−11.32	+0.06
		2016	−11.13	+0.19
		2019	−11.15	−0.02
	SS WM Barkley	2010	−13.64	–
		2015	−12.96	+0.68
		2016	−13.50	−0.54
		2019	−13.97	−0.47
Multimodal	*SS Chirripo*	2015	No erosion recorded	–
		2016	No erosion recorded	–
	SS Tiberia	2015	−4.27	–
		2016	−4.18	+0.09
	SS Polwell	2015	−1.48	–
		2016	−1.52	−0.04
		2019	−1.54	−0.02
	FV St. Michan	2015	−4.34	–
		2019	−4.47	−0.13
Gravel	*SS Lugano*	2016	No erosion recorded	–
	SS Santa Maria	2016	−5.23	–

3.3 | Time-lapse analysis

Results of the time-lapse analysis are divided into multiannual (9, 5, and 4 years), annual, and weekly changes. Table 3 contains measured maximum scour depths and their time-lapse changes, which are mostly within the detection threshold (30 cm) and are, therefore, deemed insignificant. *SS WM Barkley* is the exception, where the scour pit underwent significant (>30 cm) changes with respect to its maximum depth; however, the net change (2010–2019) was only 33 cm (Table 3). Results of the time-lapse volumetric change calculations for shipwrecks on sandy beds are listed in Table 4. The analysis for the multimodal sites does not indicate any significant volumetric changes outside detection thresholds, and no time-lapse data are available for the gravel-dominated substrate sites.

3.3.1 | Multiannual change

Multiannual difference models were created using 2010, 2015, and 2019 DEMs. Sites with major and minor changes are shown in Figures 6 and 7, respectively.

In general, the biggest changes occurred at the sand-dominated sites (Figure 6 and Table 4). At the *SS Hare* and *SS WM Barkley* sites, significant changes occurred outside and inside the dominant depositional and erosional signatures in all of the multiannual time steps. Changes at the *SS WM Barkley* site are the largest, with a maximum depth of erosion recorded at −4.9 m over a 4-year period (Figure 6b) and maximum deposition of +3.3 m for the preceding 5-year period (Figure 6a). These changes occurred in the immediate vicinity of the shipwreck, causing partial burial of its portside and partial exposure of the starboard side. A scour pit extending from the detached bow (NE part) was infilled with sediment between 2010 and 2015 (Figure 6a) and eroded again to the initial condition between 2015 and 2019 (Figure 6b). During the 9-year period, the seafloor immediately SE of the wreck structure eroded, and material was deposited further downstream (Figure 6c), resulting in a build-up of a sand mound. In terms of volumetric changes, the overall net sediment budgets calculated for the *SS WM Barkley* and *SS Hare* wreck sites in the 100-m circular buffer are negative (Table 4). At *SS Hare*, major geomorphic changes occurred between 2010 and 2015

TABLE 4 Volumetric changes for different time steps, expressed in cubic meters within the 50- to 500-m radii buffer zones around the shipwrecks

		1 week: 2019b-2019a			1 year: 2016-2015			4 years: 2019-2015			5 years: 2015-2010			9 years: 2019-2010		
Wreck	Radius	Erosion	Deposition	Net change	Erosion	Deposition	Net change	Erosion	Deposition	Net change	Erosion	Deposition	Net change	Erosion	Deposition	Net change
HMS Vanguard	50 m							-11.23	22.69	11.46						
	100 m							-47.09	174.12	127.03						
	200 m							-2575.28	4796.06	2220.78						
	300 m															
	400 m															
	500 m															
SS Hare	50 m	-0.23	0.49	**0.26**	-30.82	133.48	**102.65**	-505.20	221.82	**-283.37**	-1062.54	840.93	**-221.61**	-1523.81	918.72	**-605.09**
	100 m	-5.70	1.33	**-4.37**	-578.41	1764.14	**1185.73**	-1824.13	1375.70	**-448.43**	-2961.24	2818.04	**-143.20**	-3957.92	3463.40	**-494.52**
	200 m	-7.99	3.97	**-4.03**	-3444.22	9830.36	**6386.14**	-7604.72	8106.89	**502.17**	-9290.81	13211.29	**3920.48**	-10741.06	16810.23	**6069.17**
	300 m	-14.71	13.00	**-1.71**	-8088.05	24410.36	**16322.31**	-19561.66	20546.29	**984.63**						
	400 m				-10882.67	41934.36	**31051.69**	-28698.65	46692.15	**17993.49**						
	500 m				-13944.45	64839.67	**50895.22**	-43783.27	69741.71	**25958.44**						
SS WM Barkley	50 m	-0.68	0.47	**-0.21**	-935.32	81.39	**-853.93**	-3028.32	2.23	**-3026.09**	-2460.34	1330.30	**-1130.04**	-5042.73	185.70	**-4857.02**
	100 m	-2.63	12.10	**9.48**	-2234.40	1613.39	**-621.00**	-6699.85	2896.88	**-3802.97**	-7874.49	5242.73	**-2631.76**	-11866.02	4428.96	**-7437.05**
	200 m	-5.36	29.93	**24.57**	-7702.36	7984.55	**282.19**	-15797.30	10787.68	**-5009.62**						
	300 m				-16765.82	20671.64	**3905.81**									
	400 m				-27266.39	40097.33	**12830.94**									
	500 m															
RMS Leinster	50 m				-60.87	108.51	**47.65**	-95.84	301.77	**205.93**						
	100 m				-382.24	674.90	**292.66**	-784.22	1387.56	**603.34**						
	200 m				-2133.71	5006.53	**2872.82**	-4485.24	9396.18	**4910.94**						
	300 m															
	400 m															
	500 m															

Note: Blank cells indicate that the extent of a digital elevation model of difference did not allow for a calculation or that there are no data for the given time step. Increasing red intensity corresponds to higher deposition, whereas blue intensity indicates higher erosion.

(Figure 6d), but less extensive changes were recorded in the subsequent 4 years (Figure 6e). This is also shown in the 9-year time lapse (Figure 6f), which mostly encompasses the changes that happened during its first 5 years (between 2010 and 2015). A very sharp increase is noted in volumetric change for the *SS Hare* site between the 200 and 300-m buffers for the 2015–2019 time step, which can be attributed to the buildup of a large sediment wave located north of the wreck (Table 4 and Figure 2b).

No significant change was detected in the immediate vicinity of the wreck for the *RMS Leinster* site (Figure 6g). However, notable changes are present in the large sediment waves around the site (Figure 6g), emphasized by large volumetric changes for buffers exceeding 100-m radius (Table 4).

The 2019–2015 time-lapse analysis at the *HMS Vanguard* site (Figure 6h) shows substantial changes associated with sediment wave migration largely outside the dominant comet-shaped scour pit, which remained relatively stable with its outline clearly visible in the DoD (Figure 6h). In Table 4, this notable difference between processes inside and outside the scour pit is indicated by a significant increase in erosion/deposition values in a 200-m circular buffer around the wreck as compared with a 100-m radius buffer.

The time-lapse analysis over a 4-year period for the multimodal sites (*SS Polwell* and *FV St. Michan*) displayed a little geomorphic change (Figure 7). Almost all recorded changes at these sites are within the difference modeling detection threshold, manifested as multiple striping artifacts in the DoDs (Figure 7). Localized areas of ±0.3 m change are detected in the proximity of *SS Polwell* (Figure 7a). *FV St. Michan*'s erosional signatures exhibit a negative change reaching up to −0.3 m and a slight, localized elevation (+0.2 m) of the seabed south of the shipwreck. Retaining some pixels within the detection threshold highlights trawl marks running across the site, including one trawl mark directly intersecting the shipwreck (Figure 7b). As their linear appearance somewhat resembles striping artifacts normally occurring within the same DoD threshold, an additional examination of a multidirectional hillshade surface of the 2019 survey's DEM was performed (Majcher et al., 2020). The trawl marks are clearly manifested in the resultant hillshade raster (Figure 7c). Further evidence that these linear features are trawl marks (and not survey artifacts) is their orientation relative to the N–S orientation of the survey lines.

3.3.2 | Annual change

Annual DoDs were investigated with the 2015 and 2016 DEMs. Sites with major and minor changes are shown in Figures 8 and 9, respectively.

Similar to the multiannual time steps, the most substantial changes happened at the sand-dominated sites in terms of annual change (Figure 8). The scour pit extending from *SS WM Barkley's* detached bow is eroded further in this time step (Figure 8a), a process also manifested in the scour feature SW of the shipwreck. Data acquired over *SS WM Barkley* for this time step allowed for wider areal perimeters for volumetric calculations (Table 4), which show a substantial increase in the volumes of displaced

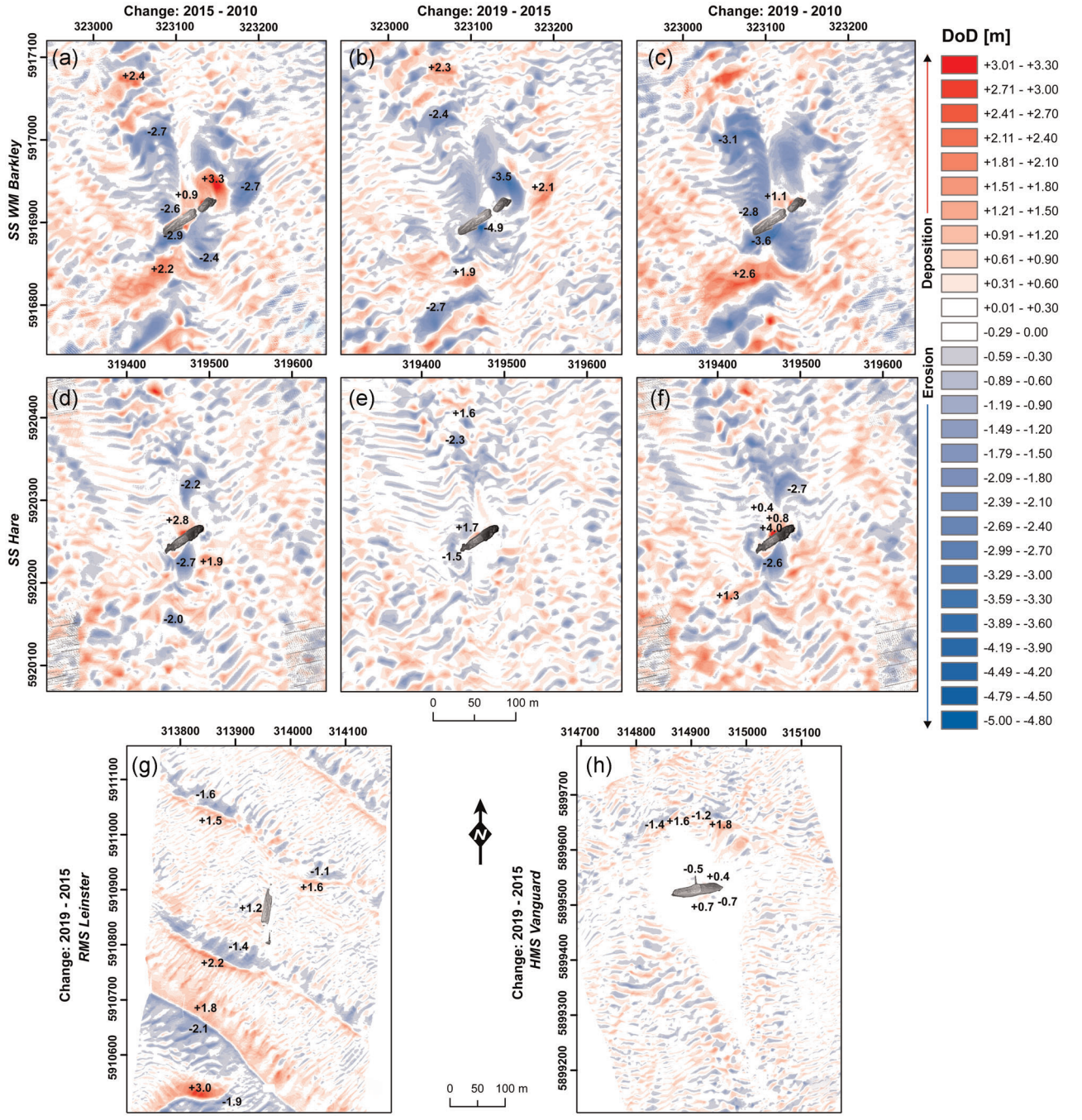

FIGURE 6 Multiannual digital elevation models of difference with major geomorphic changes for *SS WM Barkley* (a) 2015–2010, (b) 2019–2015, (c) 2019–2010; *SS Hare* (d) 2015–2010, (e) 2019–2015, (f) 2019–2010; *RMS Leinster* (g) 2019–2015; *HMS Vanguard* (h) 2019–2015. Pixels within the detection threshold (±30 cm) are in white [Color figure can be viewed at wileyonlinelibrary.com]

materials with buffers exceeding 200-m radii, especially considering deposition. A similar situation is recorded at the *SS Hare* site. This sharp increase in volumetric changes may be related to changes in the large sediment waves present north of the sites. Migration of the smaller sediment waves is visible across all the sites; however, there are differences in magnitudes in the associated changes. Sediment wave migration inside *SS Hare*'s pit is minimal near the wreck and magnified farther away from it (Figure 8b), with the farther changes manifested by increasing volumetric changes with increased buffer sizes (Table 4). The time-lapse analysis of the zone near the shipwreck does not record significant changes, with the exception of a small depositional zone (reaching +0.7 m) developed in its immediate vicinity. Sediment movement is observed everywhere around *RMS Leinster*, with changes also recorded in the large sediment waves south and north of it. Volumetric changes at the site show a similar pattern

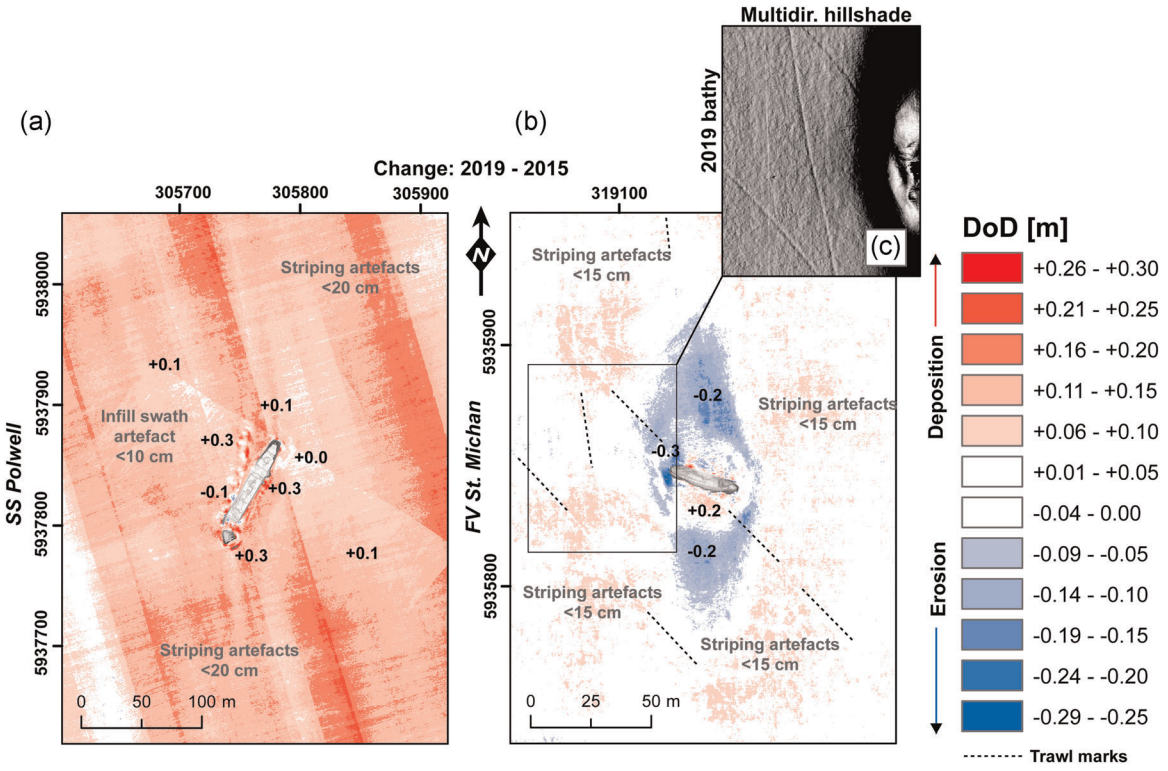

FIGURE 7 Multiannual digital elevation models (DEMs) of difference with minor geomorphic changes for (a) *SS Polwell*, 2019–2015, (b) *FV St. Michan*, 2019–2015, and (c) inset map showing a multidirectional hillshade raster created using the 2019 DEM with *FV St. Michan*. Pixels within the detection threshold (±30 cm) were retained to avoid information loss [Color figure can be viewed at wileyonlinelibrary.com]

to its multiannual change, increasing significantly with buffers in excess of 100-m radius (Table 4).

All the annual changes recorded in the DoDs at the multimodal sites are within detection thresholds and are, therefore, deemed insignificant. The 2015–2016 difference model (Figure 9a) for the *SS Chirripo* site shows virtually no change, with the positive/negative striping attributed to survey artifacts. Some areas of minor change are noted at the *SS Tiberia* shipwreck site (Figure 9b), with a similar localized change observed at the *SS Polwell* site for the same time step. Although low-profile (±0.2 m) sediment wave migration is

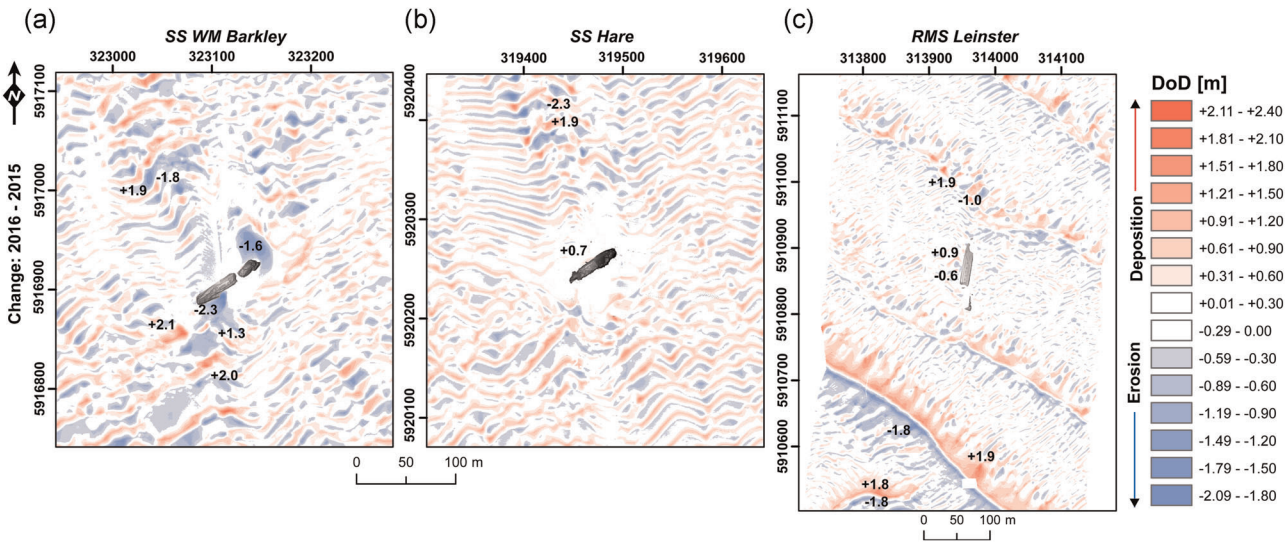

FIGURE 8 Annual digital elevation models of difference (2016–2015) with major geomorphic changes for (a) *SS WM Barkley*, (b) *SS Hare*, and (c) *RMS Leinster*. Pixels within the detection threshold (±30 cm) are in white [Color figure can be viewed at wileyonlinelibrary.com]

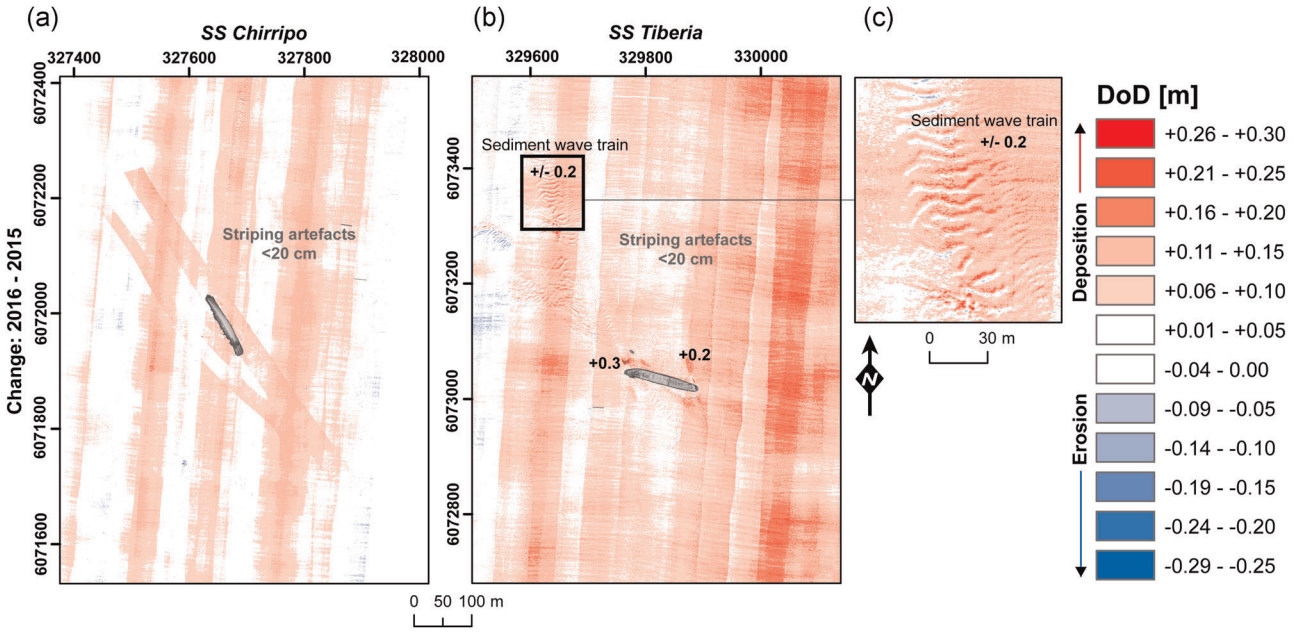

FIGURE 9 Annual digital elevation models of difference (2016–2015) with minor geomorphic changes for (a) *SS Chirripo*, (b) *SS Tiberia*, and (c) inset map showing a sediment wave train in *SS Tiberia*'s far field. Pixels within the detection threshold (±30 cm) were retained to avoid information loss [Color figure can be viewed at wileyonlinelibrary.com]

modeled far from the *SS Tiberia* site (Figure 9c), it is impossible to attribute this change directly to the presence of the shipwreck (Figure 9c).

3.3.3 | Weekly change

Difference models for a 1-week period before and after a spring tide and a coincident storm event at the *SS Polwell* site show no change. Difference models for the same period/event at the *SS WM Barkley and SS Hare* sites (Figure 10) show migrating sediment wave trains around both shipwrecks. Sediment wave migration is amplified NNE and SSW of the shipwrecks, up to 200 m from the structures. An amplified change is also visible near the SE sides of the shipwrecks, reaching ±0.3 m in the case of *SS WM Barkley* and ± 0.5 m for *SS Hare*. Survey artifacts are not aligned with the changes in the sediment waves, indicating that the observations of migration are reliable, despite being largely within the detection thresholds. Volumetric changes for this time step increase slightly with the increase in buffer size (Table 4), due to the increasing number of sediment wave changes incorporated in consecutive perimeter radii.

4 | DISCUSSION

In this study, we aimed to expand our knowledge of shipwreck site formation processes, focusing on sediment budgets and hydrodynamic conditions. To accomplish this, we investigated the spatial and temporal scales of geomorphic change at metal-hulled historic shipwrecks in a tidally dominated environment. The sites, characterized by a mosaic of seabed substrates and varying tidal currents, are all more than 100 years old; thus, their protection is endorsed by UNESCO through the Convention on the Protection of Underwater Cultural Heritage (UNESCO, 2002).

4.1 | Variability of geomorphic change at sites in different seabed environments

At all wreck sites where erosional and depositional signatures were identified, a strong correlation between their directionality and the prevalent current direction is noted, suggesting that current-induced bed stress is the dominant control on scour processes. A geomorphic change verified by difference modeling primarily takes place either inside the scour signatures or is associated with the tidally controlled migration of sediment waves. Even during storm conditions, the influence of wave action on the sites is shown to be insignificant. However, to fully determine the influence of storm events, deployment of monitoring equipment at the sites would be necessary.

4.1.1 | Sand-dominated sites

Wreck sites located in sand-dominated settings are highly dynamic, with significant changes in seabed morphology recorded on a weekly,

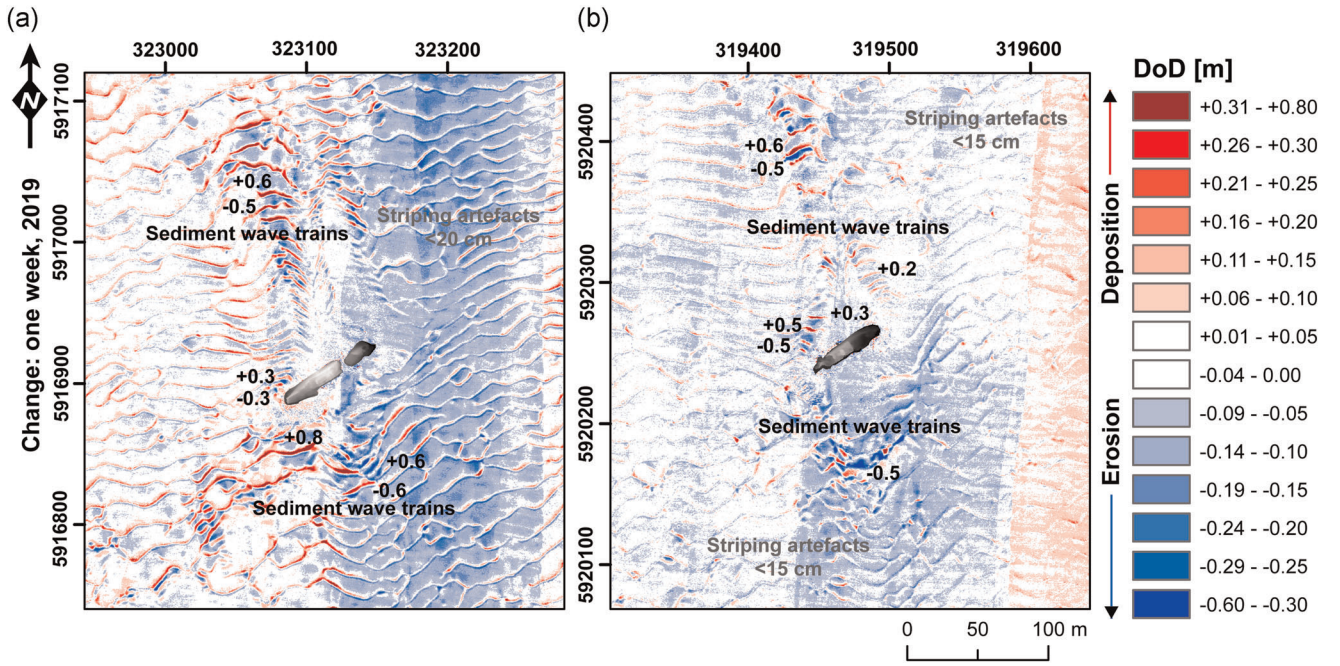

FIGURE 10 Weekly digital elevation models of difference (2019) for (a) *SS WM Barkley* and (b) *SS Hare*. Pixels within the detection threshold (30 cm) were retained to avoid information loss [Color figure can be viewed at wileyonlinelibrary.com]

annual, and interannual basis. The geomorphic change at sand-dominated sites includes the dynamic evolution of the scour pits and significant migration of sediment waves across individual wreck sites. Sediment wave trains provide a constant sediment supply, causing continued reorganization of both depositional and erosional signatures. Sediment is subsequently carried away from the sites with migrating sediment waves, which are magnified downstream of the shipwrecks. The sediment budget, therefore, fluctuates, which is reflected in the volumetric changes representing erosion and deposition at and around the sites.

Sand-dominated sites exhibit the highest and most consistent levels of bed stress values, exceeding sediment thresholds, enabling mobilization (Table 2). The stratigraphy at these sites is often complex, with quaternary sediments overlain by migrating bedforms and sand sheets controlled by contemporary hydrodynamic processes. Sediment waves in this part of the Irish Sea are typically formed in an upper mobile layer that comprises reworked glacial and postglacial sediments. Beneath this mobile layer lies a coarse gravel lag of glacial origin, either the chaotic facies or the upper till members described by Jackson et al. (1995). These Late Pleistocene layers are more resistant to scour due to their coarse composition and/or overconsolidated nature (Coughlan et al., 2020). This is demonstrated at the *HMS Vanguard* site, where a significant geomorphic change is recorded (Figure 6h), but further vertical erosion of the scour pit is limited by the presence of the underlying glacial deposits (Figure 3). Given the similarities in regional geology, it is, therefore, possible that similar limiting layers occur at the *RMS Leinster*, *SS Hare*, and *SS WM Barkley* sites. Seismic data collected at these sites are not sufficient to confirm this. Barriers limiting the vertical geomorphic change at shipwrecks have previously been postulated, for example, at the *HMS Scylla* site (investigated by Astley, 2016) or *Queen Anne's Revenge* (McNinch et al., 2006). Here, we demonstrate that such limits can be detected by shallow seismic profiling, enabling accurate predictions of future scour progression at underwater sites. This technique, therefore, provides important information for site management, allowing for more accurate underwater site formation models.

In another possible scenario for the sand-dominated sites, a limit to further vertical erosion may appear when the scour pits develop to the level at which a shipwreck will be lowered below the ambient seabed and cease to perturb the flow of tidal currents (McNinch et al., 2006; Trembanis et al., 2007). In this way, a low-lying shipwreck structure halts ongoing scour processes, so it becomes gradually buried under sediments supplied with the migrating bedforms or during quiescent periods (McNinch et al., 2006). However, the 2019 survey data indicate that all the investigated shipwrecks with deep scour pits still present significant obstructions to the tidal currents (Table 2) and do not appear to be sinking within the depressions. Hence, this scenario has a low probability, unless the shipwrecks experience dramatic structural changes that would lower their height above the seabed (Astley, 2016).

Notably, the maximum scour depths do not change significantly at any of the wreck sites investigated. The largest change in the total scour depth occurred at the *SS WM Barkley* site between the years 2010 and 2015, when one of the pits was infilled with sediment; however, the same pit was eroded again in the subsequent years (Table 3).

4.1.2 | Multimodal sites

Wrecks located in multimodal sedimentary settings are exposed to bidirectional tidal currents of similar magnitudes and exhibit an equally diverse range of geomorphic features as those located in sandy sediments. However, the multimodal sites display little or no volumetric or geomorphic change over time. This finding is important for future site predictions and reflects the advice from I. A. K. Ward et al. (1999) that although the sediment budget and hydrodynamic environment of a site are inextricably connected, they need to be examined collectively and independently to fully understand site formation processes. Although the presence of high-magnitude currents at these sites increases the potential for bedform migration, it only occurs where substrates are prone to mobility. At the multimodal sites, bedform migration is very limited. Hence, the seabed around the shipwrecks is nearly stable, without significant loss or gain in sediment budgets.

Localized areas of low-magnitude change not exceeding 30 cm at *SS Polwell* (Figure 7a) *and SS Tiberia* (Figure 9b) are attributed to fluctuating, turbulent components of flow around the shipwrecks, which locally magnify current-related shear stresses exerted on the seabed by introducing lee-wake vortices and vortex shedding (Quinn, 2006; Smyth & Quinn, 2014). The same mechanism was cited by Astley (2016) to explain localized, internal changes at the *SS Richard Montgomery* site.

At the *SS Chirripo* site, pockmark-like features are observed around the shipwreck. Their origin remains unknown; however, they could be traces of salvage operations conducted at the site in the past. Another possibility is that the impact of the shipwreck on the seabed exerted excessive pressure on the sediments, causing gas emission from the interstitials, creating the pockmarks. This formation mechanism had been hypothesized by Geraga et al. (2020) for similar morphological features at wreck sites in the Ionian Sea.

The seabed around *SS Chirripo* is also characterized by elongate depositional ridges, with no significant erosional features (Figure 4a). Despite its relative proximity (located 2.4 km to the northeast), the *SS Tiberia* site (Figure 4b) is characterized by more complex intricate patterns of erosional and depositional signatures. Differences in scour patterns at the two proximal sites are attributed to higher peak current values and subsequent higher levels of sediment threshold exceedance for mobilization at the *Tiberia* site. This influence is also reflected in the migration of low-profile sediment waves nearby the site (Figure 9c). Additionally, *SS Chirripo* is orientated oblique (nearly parallel) to the dominant currents, hence perturbing flow to a far lesser extent than *SS Tiberia*, whose full length is oriented nearly perpendicular to the peak flow (Quinn & Smyth, 2018).

Local geological control on scour signature propagation is also observed at the multimodal *SS Polwell* site. Although extensive scour is recorded to the north of the wreck, scouring to the south of the structure is limited (Figure 4c), despite a strong bidirectional current flow. A distinctive ridge feature located to the south acts as a horizontal (or spatial) impediment to scour propagation. Given its morphology and the regional geology, this ridge is likely to be a surface or near-surface expression of the chaotic facies or upper till member.

Difference modeling for the *FV St. Michan* site shows that the low-magnitude change is confined almost entirely to the scour pit (Figure 7b), suggesting that the flows magnified by the shipwreck are still eroding the seafloor. The analysis of grab samples collected at the site indicate highly multimodal sediments, as the shipwreck rests on the rim of the Western Irish Sea Mud Belt. The sediments in this area, the mud facies of Jackson et al. (1995), are typically underconsolidated with low shear strength values and are prone to scour (Callaway et al., 2009; Coughlan et al., 2019). Furthermore, mobilization and removal of fine-grained sediments in this area of the Irish Sea have been shown to be exacerbated by commercial trawling activity, which is clearly evidenced at the *St. Michan* site in Figure 7c (Coughlan et al., 2015).

4.1.3 | Gravel-dominated sites

Although no time-lapse data of sufficient resolution are available for the gravel-dominated sites, MBES coverage and sediment samples, coupled with modeled near-seabed current information, allow for some observations. For example, at the *SS Santa Maria* site located off the north coast of Ireland, a significant volume of material has been eroded from around the bow of the wreck (Figure 5b and Table 2), and it is the only site where no deposition of sediment is recorded. The complex bathymetry of the site makes it difficult to differentiate shipwreck-related geomorphological features from those developed naturally, even after applying a residual relief modeling approach to site characterization (Majcher et al., 2020). In contrast, high-resolution MBES data from the nearby *SS Lugano* site display no erosion, despite predictions from amplified shear stress calculations. This is attributed to the shipwreck's more streamlined orientation with respect to the dominant flow, analogous to the *SS Chirripo* case described above. The geometry of the depositional signatures recorded at the *Lugano* site matches the computational fluid dynamics-derived predictions of Quinn and Smyth (2018) for shipwrecks oriented parallel to the peak flow.

4.1.4 | Discrepancies between modeled and observed data

Discrepancies are noted between the predictions of the sediment transport models and direct, time-lapse observations at some of the wreck sites in the study. No significant geomorphic change is recorded at the multimodal sites, even though the sediment mobility thresholds are frequently exceeded (Table 2). These differences may be explained by the oversimplified nature of some sediment transport models that do not account for multimodality of sediments, leading to a substantial influence on calculating the critical shear stresses required to mobilize sediment. For example, at the *SS Polwell* site, a mud–sand–gravel mixture is observed inside the erosional

signature. According to McCarron et al. (2019), the critical shear stress needed to mobilize sand–gravel sediments may be decreased by 64% and increased by 75% for gravel and sand, respectively, when a hiding and exposure effect resulting from bimodality is introduced. Hence, it is possible that this effect resulted in finer sediments being removed from multimodal substrates at the *SS Tiberia*, *FV St. Michan*, and *SS Polwell* sites, leaving behind a coarser lag that is resistant to scour. The calculated volumes of erosion and deposition at these sites are similar (Table 2), suggesting that the eroded material may have been redeposited further downstream from the shipwrecks. It is, therefore, proposed that the absence of time-lapse change at the sites where the obstacle-amplified shear stresses exceed mobility thresholds can be also attributed to the effects caused by the multimodality of sediments.

4.2 | Equilibrium states of shipwrecks and their implications for in situ preservation

It is clear that sand-dominated sites are highly dynamic as compared with the gravel-dominated and multimodal sites (Figure 11a). This dynamism is manifested in all aspects of the sites' analyses, from the initial volumes calculated for the erosional and depositional signatures, through volumetric changes and changes detected in the DoD. The continuous migration of sediment waves through the *SS WM Barkley*, *SS Hare*, and *RMS Leinster* sites triggers a frequent reorganization of material around the shipwrecks, which, in turn, causes them to shift from one equilibrium state to another. Such shifts may possibly be triggered on a weekly basis during spring tides, as a significant wave migration is recorded even in the shortest time step. These wrecks are not only affected by the constant external supply of sediment, but also by active scour processes, expressed by the negative net sediment budget in their 100-m circular buffers for multiannual surveys (Table 4). Similar to the *Burgzand Noord* shipwrecks in the North Sea described by Manders (2009) and Astley (2016), the sites in the Irish Sea undergo material loss. However, whereas the *Burgzand Noord* sites remain structurally unaffected by this change, the integrity of *SS Hare* and *SS WM Barkley* may be threatened in the longer term, as large volumes of sediments are constantly reorganized in their immediate surroundings.

The dynamism at these sites is more analogous to the *HMS Stirling Castle* wreck site, also located in the North Sea, where a constant sediment supply due to sandbank migration regularly causes a significant geomorphic change, resulting in repeated burial and exposure of the shipwreck (Bates et al., 2011; Pascoe, 2012). Significant changes (±2–3 m) on a multiannual timescale were also noted at the more modern (World War 2) shipwreck site of *SS Richard Montgomery* (Astley, 2016). The wreck is also situated on a sandy seabed (fine sand), with an external supply of sediments, and the reorganization of the erosional/depositional signatures was observed around it (Astley, 2016).

Such an open, high-energy system may have a profound impact on in situ preservation of archaeological material. Tonnes of sediments are regularly eroded/deposited around the shipwrecks, acting as scrambling devices (Muckelroy, 1978) and causing rapid shifts in pressures acting on their hulls. This mechanism probably affects the *SS WM Barkley* site. In the time-lapse data we collected, a build-up of sediment is initially recorded to the north of the shipwreck, partly covering its portside (years 2010–2015; Figure 6a). Subsequently, substantial erosion of the site uncovered part of its starboard side (years 2015–2019; Figure 6b). This erosion event also gave rise to the maximum bathymetric change (−4.9 m) recorded in any of the DoD. Such dramatic bed level change is likely to impact the structural stability of shipwrecks, resulting in mechanical damage and accelerated collapse (Quinn, 2006). Therefore, such open sites, in highly dynamic equilibrium with their environment, should be a priority when it comes to introducing in situ preservation measures, planning regular monitoring or authorized emergency excavation.

An exception among the sand-dominated wrecks is the *HMS Vanguard* site, where scouring appears to have reached its maximum depth. A non-erodible coarser sediment layer exposed in the scour pit limits the vertical scour extent and sediment wave migration occurs only outside of it. As sediment supply to the site has ended, the site appears to have reached a static equilibrium phase (Figure 11a). This stability has possibly aided the remarkable preservation of the shipwreck, despite it being older than the other sites investigated. *HMS Vanguard* is nearly fully intact on the seabed in comparison to the other sand-dominated sites (Table 2), which are partly buried and scattered. Although the site appears stable, change may be triggered in the future by events like severe storms, anthropogenic activities, or parts of the wreck itself collapsing (Figure 11a). *HMS Vanguard* is still in a negative disequilibrium trend like any other underwater site and will undergo a gradual degradation due to corrosion and other formation processes, as it is almost entirely exposed to the seawater (I. A. K. Ward et al., 1999; Figure 11c).

The sites dominated by multimodal sediments expressed virtually no significant geomorphic change throughout all the time-lapse periods, and may, therefore, be described as static, closed systems, which have achieved a stable equilibrium (Figure 11b). These shipwrecks are only slightly buried in the seabed, and the scour processes have settled analogous to artificial reef structures on a mixed seafloor described by Raineault et al. (2013). At the *SS Tiberia*, *FV St. Michan*, and *SS Polwell* sites, scour processes caused the removal of fine-grained sediments, leaving only coarser, non-erodible substrates in the pits. *SS Chirripo* must have reached the equilibrium state soon after the wrecking incident, as no scour is recorded around it. As a result, these shipwrecks are generally largely intact and have a higher preservation potential, akin to *HMS Vanguard*.

Although no time-lapse data are available for the *SS Lugano* site, it is also assumed to be in a static equilibrium with the environment. No erosion is recorded in the DEM (Figure 5a) and no sediment waves are present; thus, the geomorphological context is assumed static. However, *SS Santa Maria*'s broken bow caused the advance of significant erosional signatures (Figure 5b), despite resting on a coarse seabed dominated by gravel and boulders. The tidal currents

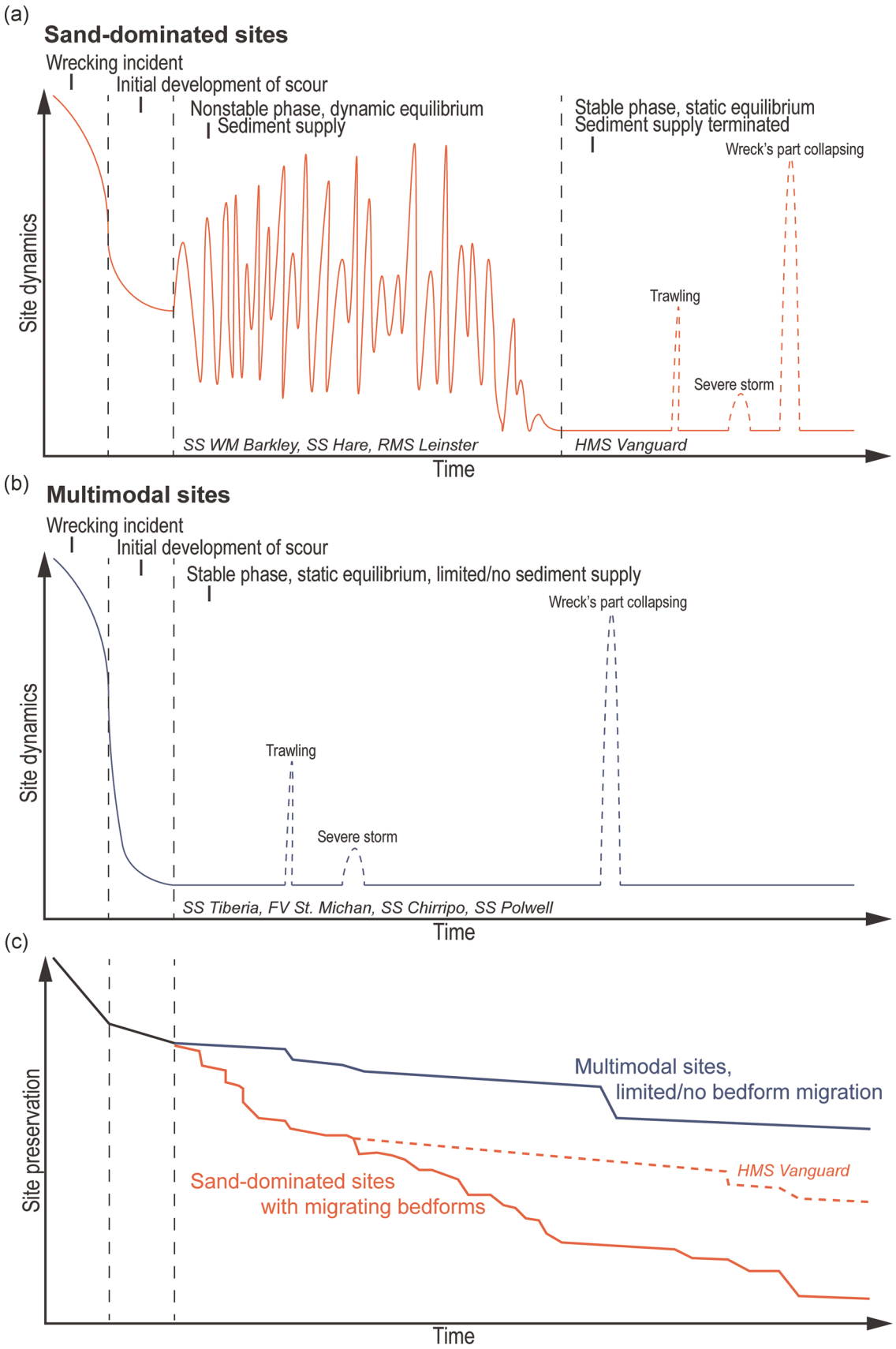

FIGURE 11 Conceptual site dynamics models for the investigated sand-dominated (a) and multimodal sites (b) with a corresponding site preservation estimation for the two categories (c). Rapid changes in the site dynamics due to continuous sediment supply and/or single events cause accelerated degradation and lower site preservation. In contrast, stable periods favor preservation, which is, however, always decreasing due to chemical and biological deterioration [Color figure can be viewed at wileyonlinelibrary.com]

at the location are among the strongest in the Irish Sea (Pérez-Ortiz et al., 2017); hence, there is a probability of some geomorphic change and the associated system's instability.

Nevertheless, it is important to understand that the stability of underwater sites is not solely controlled by their geomorphological and hydrodynamic settings. A disruption of any equilibrium state can be triggered by external anthropologic influences like digging (Manders, 2009), trawling (Brennan et al., 2016), or dredging operations (Quinn & Boland, 2010). In this study, a direct indication that anthropogenic activity impacts the sites is evidenced by the trawl marks at *FV St. Michan*. Although no obvious significant reorganization of material has occurred at that site, it is possible that continuation of the trawling may damage the shipwreck and trigger further changes as new nuclei for scour may be introduced, increasing site dynamics (Figure 11b; Quinn, 2006).

In summary, we suggest that knowledge about sediment types, bathymetry, and hydrodynamic processes at underwater sites can provide invaluable information for cultural resource managers. More important, such high-quality hydrographic, oceanographic, and geological data are becoming increasingly publicly available through various studies, initiatives, and projects like INFOMAR in Ireland (Guinan et al., 2020; O'Toole et al., 2020). Such open-sourced data sets can be used for pilot studies, assessing the preservation potential of individual sites and targeting the shipwrecks that need more detailed investigation, for example, involving high-resolution time-lapse surveys.

Further research is needed in understanding vertical propagation of scour at shipwreck sites, for example, using shallow seismic profiling, which is proven to be an effective method for detecting limiting horizons. Studies of internal reorganization of scour pits and depositional signatures caused by the external supply of sediments through migrating bedforms need to be investigated in greater detail, to understand how these two processes are related. Future sediment budget investigations should also include multimodality effects on sediment mobility at sites (McCarron et al., 2019).

Although we successfully investigated the geomorphic change at shipwreck sites at weekly, annual, and multiannual time steps, these time series should be extended at both ends, allowing the capture of very short-term (daily tidal oscillations and storms) and long-term (10+ years) changes at sites. Additionally, we recognize the need to evaluate the direct influence of dynamic geomorphic change on the structural integrity of shipwrecks. Although such geomorphic changes are known to have detrimental effects on frequently monitored offshore engineering structures (Melling, 2015; Whitehouse et al., 2011), the scale of potential damage to historic shipwrecks remains unclear. Filling these knowledge gaps would result in further refinements of shipwreck site formation models.

5 | CONCLUSIONS

This study offers new knowledge about site formation processes and long-term stability of metal-hulled shipwrecks, which have remained largely unresearched (Keith, 2016), despite their increasing archaeological value. The management of such shipwrecks is at the crossroads of diverse interests and factors, arising from cultural heritage management, environmental risks, sport diving accessibility, and others (Firth, 2018; Tomalin et al., 2000). As geomorphic changes at the sites are demonstrated to have a direct link to their in situ preservation, we recognize this investigation as highly pertinent to support site management decisions. In the end, it is also applicable for informing future offshore developments and marine spatial planning, as shipwreck sites can be inversely used as proxies of local geomorphological and hydrodynamic conditions (Caston, 1979; Geraga et al., 2020).

ACKNOWLEDGMENTS

The authors specially thank Andrew Conway and the MI Oceanographic Services Team for their assistance with the ocean current data compilation. They thank the reviewers and the associate editor for their insights, which helped them to improve the manuscript. They would also like to thank Carlos Loureiro for advice regarding the buoy data. Additionally, they express their gratitude to Alex Braun, Annika Clements, Shauna Creane, Mekayla Dale, Eoghan Daly, Megan Dolan, Cristiana Giglio, Rory McNeary, Rory O'Loughlin, Kevin Sheehan, and Viacheslav Sobolev for their help with the hydrographic and seismic data acquisition and processing, to Cynthia Sassenroth and Mary Therese Kelly for processing the sediment samples and finally to the crew of *RV Celtic Voyager* for their passion and never-ending patience when surveying the wrecks. This study was supported by the Marine Institute of Ireland's ship-time programme's APP-CV15021, CV16031: *World War I shipwrecks in the Irish Sea: commemoration, visualization and heritage management*, APP-CV19027: *Geohazard investigation in the Irish Sea using seismic and seabed mapping techniques* (GIST), Ulster University Vice-Chancellor's Research Studentships and *the Integrated Mapping for the Sustainable Development of Ireland's Marine Resource* (INFOMAR) programme's surveys CV10_01, CV09_05, CV08_03. Open access funding enabled and organized by Projekt DEAL.

CONFLICT OF INTERESTS

The authors declare that there are no conflict of interests.

DATA AVAILABILITY STATEMENT

The bathymetric and seismic data that support the findings of this study are available upon request from the corresponding author at Ulster University, INFOMAR program (https://www.infomar.ie/) and the Marine Institute of Ireland (https://www.marine.ie/). The sediment sample data are available as mean sediment grain size values in the Supporting Information for this paper available under the link: https://doi.org/10.17605/OSF.IO/5C4QX. ROMS current data were supplied by the Oceanographic Services team within Ocean Science and Information Services division of the Marine Institute (Ireland), and the M2 buoy data were downloaded from data.gov.ie (Copyright Met Éirean, source, published under a Creative Commons Attribution 4.0 International, CC BY 4.0).

ORCID

Jan Majcher http://orcid.org/0000-0003-2894-6423
Rory Quinn http://orcid.org/0000-0001-7946-565X
Ruth Plets http://orcid.org/0000-0002-9092-7533
Mark Coughlan http://orcid.org/0000-0003-2216-7883
Christopher McGonigle http://orcid.org/0000-0002-0262-0559
Fabio Sacchetti http://orcid.org/0000-0002-2098-7071
Kieran Westley http://orcid.org/0000-0002-0863-6762

REFERENCES

Astley, A. J. (2016). *The taphonomy of historic shipwreck sites* (doctoral thesis). University of Southampton, Ocean and Earth Science. http://eprints.soton.ac.uk/id/eprint/402317

Atkins, W. S. (1997). Chapter 2.3: Wind and water. In J. P. Doody, N. C. Davidson, J. H. Barne, C. F. Robson, S. S. Kaznowska, & A. L. Buck (Eds.), *Coasts and seas of the United Kingdom, Region 17: Northern Ireland* (pp. 28–32). Joint Nature Conservation Committee. (Coastal Directories Series).

Bałazy, P., Copeland, U., & Sokołowski, A. (2019). Shipwrecks and underwater objects of the southern Baltic—Hard substrata islands in the brackish, soft bottom marine environment. *Estuarine, Coastal and Shelf Science*, *225*, 106240. https://doi.org/10.1016/j.ecss.2019.05.022

Bates, C. R., Lawrence, M., Dean, M., & Robertson, P. (2011). Geophysical methods for wreck-site monitoring: The Rapid Archaeological Site Surveying and Evaluation (RASSE) programme. *International Journal of Nautical Archaeology*, *40*(2), 404–416. https://doi.org/10.1111/j.1095-9270.2010.00298.x

Belderson, R. H. (1964). Holocene sedimentation in the western half of the Irish Sea. *Marine Geology*, *2*(1–2), 147–163. https://doi.org/10.1016/0025-3227(64)90032-5

Bethencourt, M., Fernández-Montblanc, T., Izquierdo, A., González-Duarte, M. M., & Muñoz-Mas, C. (2018). Study of the influence of physical, chemical and biological conditions that influence the deterioration and protection of Underwater Cultural Heritage. *Science of the Total Environment*, *613–614*, 98–114. https://doi.org/10.1016/j.scitotenv.2017.09.007

Blott, S. J., & Pye, K. (2001). Gradistat: A grain size distribution and statistics package for the analysis of unconsolidated sediments. *Earth Surface Processes and Landforms*, *26*(11), 1237–1248. https://doi.org/10.1002/esp.261

Bowden, K. F. (1980). Chapter 12: Physical and dynamical oceanography of the Irish Sea. In F. T. Banner, M. B. Collins, & K. S. Massie (Eds.), *Elsevier oceanography series* (Vol. 24, Part B, pp. 391–413). Elsevier. https://doi.org/10.1016/S0422-9894(08)71357-6

Brady, K., McKeon, C., Lyttleton, J., & Lawler, I. (2012). *Warships, U-boats & liners—A guide to shipwrecks mapped in Irish waters*. The Stationery Office.

Brasington, J., Langham, J., & Rumsby, B. (2003). Methodological sensitivity of morphometric estimates of coarse fluvial sediment transport. *Geomorphology*, *53*(3–4), 299–316. https://doi.org/10.1016/S0169-555X(02)00320-3

Brennan, M. L., Davis, D., Ballard, R. D., Trembanis, A. C., Vaughn, J. I., Krumholz, J. S., Delgado, J. P., Roman, C. N., Smart, C., Bell, K. L. C., Duman, M., & DuVal, C. (2016). Quantification of bottom trawl fishing damage to ancient shipwreck sites. *Marine Geology*, *371*, 82–88. https://doi.org/10.1016/j.margeo.2015.11.001

Brennan, M. L., Davis, D., Roman, C., Buynevich, I., Catsambis, A., Kofahl, M., Ürkmez, D., Ian Vaughn, J., Merrigan, M., & Duman, M. (2013). Ocean dynamics and anthropogenic impacts along the southern Black Sea shelf examined through the preservation of pre-modern shipwrecks. *Continental Shelf Research*, *53*, 89–101. https://doi.org/10.1016/j.csr.2012.12.010

Calder, B., & Wells, D. (2006). *CUBE User's Manual*. Durham: University of New Hampshire. http://ccom.unh.edu/sites/default/files/publications/Calder_07_CUBE_User_Manual.pdf

Callaway, A., Smyth, J., Brown, C. J., Quinn, R., Service, M., & Long, D. (2009). The impact of scour processes on a smothered reef system in the Irish Sea. *Estuarine, Coastal and Shelf Science*, *84*(3), 409–418. https://doi.org/10.1016/j.ecss.2009.07.011

Caston, G. F. (1979). Wreck marks: Indicators of net sand transport. *Marine Geology*, *33*(3–4), 193–204. https://doi.org/10.1016/0025-3227(79)90080-X

Coughlan, M., Long, M., & Doherty, P. (2020). Geological and geotechnical constraints in the Irish Sea for offshore renewable energy. *Journal of Maps*, *16*(2), 420–431. https://doi.org/10.1080/17445647.2020.1758811

Coughlan, M., Wheeler, A. J., Dorschel, B., Long, M., Doherty, P., & Mörz, T. (2019). Stratigraphic model of the Quaternary sediments of the Western Irish Sea Mud Belt from core, geotechnical and acoustic data. *Geo-Marine Letters*, *39*, 223–237. https://doi.org/10.1007/s00367-019-00569-z

Coughlan, M., Wheeler, A. J., Dorschel, B., Lordan, C., Boer, W., Gaever, P., Haas, H., & Mörz, T. (2015). Record of anthropogenic impact on the Western Irish Sea mud belt. *Anthropocene*, *9*, 56–69. https://doi.org/10.1016/j.ancene.2015.06.001

Croome, A. (1999). Sinking fast. In D. Rhind (Ed.), *Marine industrial technology* (1st and 2nd ed.). United Nations Industrial Development Organization (UNIDO).

Cvikel, D., Grøn, O., & Boldreel, L. O. (2017). Detecting the Ma'agan Mikhael B shipwreck. *Underwater Technology*, *34*(2), 93–98. https://doi.org/10.3723/ut.34.093

Delgado, J., & Varmer, O. (2015). The public importance of World War I shipwrecks: Why a state should care and the challenges of protection. In *Underwater Cultural Heritage from World War I, Proceedings of the Scientific Conference on the Occasion of the Centenary of World War I Bruges, Belgium, 26 and 27 June, 2014* (pp. 105–116).

Elkin, D., Gutiérrez, G., & Underwood, C. J. (2020). Metal shipwrecks in Patagonia, Argentina: Contributions to their research and management. *International Journal of Nautical Archaeology*, *49*(2), 303–317. https://doi.org/10.1111/1095-9270.12441

EMODnet Bathymetry Consortium. (2018). EMODnet Digital Bathymetry (DTM 2018). EMODnet Bathymetry Consortium. https://doi.org/10.12770/18ff0d48-b203-4a65-94a9-5fd8b0ec35f6

Eriksson, N., & Rönnby, J. (2012). 'The Ghost Ship'. An intact fluyt from c. 1650 in the middle of the Baltic Sea. *International Journal of Nautical Archaeology*, *43*(2), 350–361. https://doi.org/10.1111/j.1095-9270.2012.00342.x

Ferentinos, G., Fakiris, E., Christodoulou, D., Geraga, M., Dimas, X., Georgiou, N., Kordella, S., Papatheodorou, G., Prevenios, M., & Sotiropoulos, M. (2020). Optimal sidescan sonar and subbottom profiler surveying of ancient wrecks: The 'Fiskardo' wreck, Kefallinia Island, Ionian Sea. *Journal of Archaeological Science*, *113*, 105032. https://doi.org/10.1016/j.jas.2019.105032

Fernández-Montblanc, T., Izquierdo, A., Quinn, R., & Bethencourt, M. (2018). Waves and wrecks: A computational fluid dynamic study in an underwater archaeological site. *Ocean Engineering*, *163*, 232–250. https://doi.org/10.1016/j.oceaneng.2018.05.062

Fernández-Montblanc, T., Quinn, R., Izquierdo, A., & Bethencourt, M. (2016). Evolution of a shallow water wave-dominated shipwreck site: Fougueux (1805), Gulf of Cadiz. *Geoarchaeology*, *31*(6), 487–505. https://doi.org/10.1002/gea.21565

Firth, A. (2018). *Managing shipwrecks*. Fjord Limited for Honor Frost Foundation.

Foecke, T., Ma, L., Russell, M. A., Conlin, D. L., & Murphy, L. E. (2010). Investigating archaeological site formation processes on the battleship USS Arizona using finite element analysis. *Journal of*

Archaeological Science, *37*(5), 1090–1101. https://doi.org/10.1016/j.jas.2009.12.009

Folk, R. L. (1954). The distinction between grain size and mineral composition in sedimentary rock. *The Journal of Geology*, *62*(4), 344–359. http://www.jstor.org/stable/30065016

Forsythe, W., Breen, C., Callaghan, C., & McConkey, R. (2000). Historic storms and shipwrecks in Ireland: A preliminary survey of severe synoptic conditions as a causal factor in underwater archaeology. *International Journal of Nautical Archaeology*, *29*(2), 247–259. https://doi.org/10.1006/ijna.2000.0313

Frost, H. (1961). The annual lecture 1961. *The Mariner's Mirror*, *48*(2), 82–89. https://doi.org/10.1080/00253359.1962.10657686

Garlan, T., Marches, E., & Brenon, E. (2015). A classification of scouring marks in macrotidal environments from analysis of long term wreck marks. In P. Wang, J. D. Rosati, & J. Cheng (Eds.), *The proceedings of the coastal sediments 2015* (p. 14). World Scientific. https://doi.org/10.1142/9789814689977_0202

Geraga, M., Christodoulou, D., Eleftherakis, D., Papatheodorou, G., Fakiris, E., Dimas, X., Georgiou, N., Kordella, S., Prevenios, M., Iatrou, M., Zoura, D., Kekebanou, S., Sotiropoulos, M., & Ferentinos, G. (2020). Atlas of shipwrecks in Inner Ionian Sea (Greece): A remote sensing approach. *Heritage*, *3*(4), 1210–1236. https://doi.org/10.3390/heritage3040067

Gibbs, M. (2006). Cultural site formation processes in maritime archaeology: Disaster response, salvage and Muckelroy 30 years on. *International Journal of Nautical Archaeology*, *35*(1), 4–19. https://doi.org/10.1111/j.1095-9270.2006.00088.x

Gregory, D. (2020). Characterizing the preservation potential of buried marine archaeological sites. *Heritage*, *3*(3), 838–857. https://doi.org/10.3390/heritage3030046

Gregory, D., Eriksen, A. M., Pedersen, R., Jensen, P., Andersen, M. H., Davidde, B., & Smith, B. (2014). Development of tools and techniques to survey, assess, stabilise, monitor and preserve underwater archaeological sites: SASMAP, a European research project. In J. Bridgland (Ed.), *ICOM-CC 17th Triennal Conference Preprints* (p. 7). International Council of Museums. https://doi.org/10.13140/RG.2.1.4049.3926

Grøn, O., Boldreel, L. O., Cvikel, D., Kahanov, Y., Galili, E., Hermand, J. P., Nævestad, D., & Reitan, M. (2015). Detection and mapping of shipwrecks embedded in sea-floor sediments. *Journal of Archaeological Science: Reports*, *4*, 242–251. https://doi.org/10.1016/j.jasrep.2015.09.005

Guinan, J., McKeon, C., O'Keeffe, E., Monteys, X., Sacchetti, F., Coughlan, M., & Nic Aonghusa, C. (2020). INFOMAR data in the EMODnet Geology data portal supports marine spatial planning and offshore energy development in the Irish offshore. *Quarterly Journal of Engineering Geology and Hydrogeology*, *54*(1), qjegh2020-033. https://doi.org/10.1144/qjegh2020-033

Horsburgh, K. J., & Hill, A. E. (2003). A three-dimensional model of density-driven circulation in the Irish Sea. *Journal of Physical Oceanography*, *33*(2), 343–365.

Howarth, M. J. (2001). *Hydrography of the Irish Sea. SEA6 Technical Report, POL Internal Document 174*. https://assets.publishing.service.gov.uk/government/uploads/system/uploads/attachment_data/file/197294/SEA6_Hydrography_POL.pdf

IHO. (2020). *IHO Standards for Hydrographic Surveys*. https://iho.int/uploads/user/pubs/Drafts/S-44_Edition_6.0.0-Final.pdf

Jackson, D. I., Jackson, A. A., Evans, D., Wingfield, R. T. R., Barnes, R. P., & Arthur, M. J. (1995). *United Kingdom offshore regional report: The geology of the Irish Sea*. British Geological Survey.

Johnson, K. H., Paxton, A. B., Taylor, J. C., Hoyt, J., McCord, J., & Hoffman, W. (2020). Extracting ecological metrics from archeological surveys of shipwrecks using submersible video and laser-line scanning. *Emerging Technologies*, *11*(11):e03210. https://doi.org/10.1002/ecs2.3210

Keith, M. E. (2016). The role of site formation in shipwreck archaeology. In M. E. Keith (Ed.), *Site formation processes of submerged shipwrecks* (pp. 259–263). University Press of Florida.

Knight, P. J., & Howarth, M. J. (1999). The flow through the North Channel of the Irish Sea. *Elsevier Oceanography Series*, *19*, 693–716. https://doi.org/10.1016/S0278-4343(98)00110-1

Landquist, H., Hassellöv, I. M., Rosén, L., Lindgren, J. F., & Dahllöf, I. (2013). Evaluating the needs of risk assessment methods of potentially polluting shipwrecks. *Journal of Environmental Management*, *119*, 85–92. https://doi.org/10.1016/j.jenvman.2012.12.036

Lewis, M., Neill, S. P., Robins, P. E., & Hashemi, M. R. (2015). Resource assessment for future generations of tidal-stream energy arrays. *Energy*, *83*, 403–415. https://doi.org/10.1016/j.energy.2015.02.038

Majcher, J., Plets, R., & Quinn, R. (2020). Residual relief modelling: Digital elevation enhancement for shipwreck site characterisation. *Archaeological and Anthropological Sciences*, *12*(6), 122. https://doi.org/10.1007/s12520-020-01082-6

Manders, M. (2009). Multibeam recording as a way to monitor shipwreck sites. In *Managing Cultural Heritage Underwater (MACHU) Final Report NR*. Vol. 3 (pp. 59–66).

Matulla, C., Schöner, W., Alexandersson, H., Storch, H., & Wang, X. L. (2008). European storminess: Late nineteenth century to present. *Climate Dynamics*, *31*(2–3), 125–130. https://doi.org/10.1007/s00382-007-0333-y

Matutano, C., Negro, V., López-Gutiérrez, J. S., & Esteban, M. D. (2013). Scour prediction and scour protections in offshore wind farms. *Renewable Energy*, *57*, 358–365. https://doi.org/10.1016/j.renene.2013.01.048

MCA. (2016). UK Hydrography Programme. *Survey Specification*. Southampton. https://www.channelcoast.org/ccoresources/specificationsandbriefs/CHP_Survey_Specification_v2016_02.pdf

McCarron, C. J., Van Landeghem, K. J. J., Baas, J. H., Amoudry, L. O., & Malarkey, J. (2019). The hiding-exposure effect revisited: A method to calculate the mobility of bimodal sediment mixtures. *Marine Geology*, *410*, 22–31. https://doi.org/10.1016/j.margeo.2018.12.001

McNinch, J. E., Wells, J. T., & Trembanis, A. C. (2006). Predicting the fate of artefacts in energetic, shallow marine environments: An approach to site management. *International Journal of Nautical Archaeology*, *35*(2), 290–309. https://doi.org/10.1111/j.1095-9270.2006.00105.x

Mellet, C. L., Long, D., & Carter, G. (2015). *Geology of the seabed and shallow subsurface: The Irish Sea*. British Geological Survey.

Melling, G. (2015). *Hydrodynamic and geotechnical control of scour around offshore monopiles* (doctoral thesis). University of Southampton, Ocean and Earth Science.

Muckelroy, K. (1978). *Maritime archaeology*. Cambridge University Press.

Nagy, H., Lyons, K., Nolan, G., Cure, M., & Dabrowski, T. (2020). A regional operational model for the North East Atlantic: Model configuration and validation. *Journal of Marine Science and Engineering*, *8*(9), 673. https://doi.org/10.3390/jmse8090673

Neill, S. P., Hashemi, M. R., & Lewis, M. J. (2014). Optimal phasing of the European tidal stream resource using the greedy algorithm with penalty function. *Energy*, *73*, 997–1006. https://doi.org/10.1016/j.energy.2014.07.002

Ødegård, Ø., Hansen, R. E., Singh, H., & Maarleveld, T. J. (2018). Archaeological use of Synthetic Aperture Sonar on deepwater wreck sites in Skagerrak. *Journal of Archaeological Science*, *89*, 1–13. https://doi.org/10.1016/j.jas.2017.10.005

O'Shea, J. (2002). The archaeology of scattered wreck-sites: Formation processes and shallow water archaeology in western Lake Huron. *The International Journal of Nautical Archaeology*, *31*(2), 211–227. https://doi.org/10.1006/ijna.2002.1044

O'Toole, R., Judge, M., Sachetti, F., Furey, T., Mac Craith, E., Sheehan, K., & Monteys, X. (2020). *Mapping Ireland's coastal, shelf and deep water environments using illustrative case studies to highlight the impact of seabed mapping on the generation of blue knowledge*. Geological Society, London, Special Publications. https://doi.org/10.1144/sp505-2019-207

Ozer, J., Legrand, S., Od, R., & Mumm, N. (2015). *BEAWARE II: Review of the physical oceanography in the area of the Bonn Agreement*. https://www.bonnagreement.org/site/assets/files/17082/rep_2_beaware2_physicaloceanographyreport_v1_0.pdf

Pascoe, D. (2012). Samuel Pepys's navy preserved in situ? *Conservation and Management of Archaeological Sites*, *14*(1–4), 182–192. https://doi.org/10.1179/1350503312Z.00000000015

Pérez-Ortiz, A., Borthwick, A. G. L., McNaughton, J., & Avdis, A. (2017). Characterization of the tidal resource in Rathlin Sound. *Renewable Energy*, *114*, 229–243. https://doi.org/10.1016/j.renene.2017.04.026

Plets, R. M. K., Dix, J. K., Adams, J. R., Bull, J. M., Henstock, T. J., Gutowski, M., & Best, A. I. (2009). The use of a high-resolution 3D Chirp sub-bottom profiler for the reconstruction of the shallow water archaeological site of the Grace Dieu (1439), River Hamble, UK. *Journal of Archaeological Science*, *36*(2), 408–418. https://doi.org/10.1016/j.jas.2008.09.026

Plets, R. M. K., Quinn, R., Forsythe, W., Westley, K., Bell, T., Benetti, S., McGrath, F., & Robinson, R. (2011). Using multibeam echo-sounder data to identify shipwreck sites: Archaeological assessment of the Joint Irish Bathymetric Survey data. *International Journal of Nautical Archaeology*, *40*(1), 87–98. https://doi.org/10.1111/j.1095-9270.2010.00271.x

Pournou, A. (2017). Assessing the long-term efficacy of geotextiles in preserving archaeological wooden shipwrecks in the marine environment. *Journal of Maritime Archaeology*, *13*, 1–14. https://doi.org/10.1007/s11457-017-9176-9

Quinn, R. (2006). The role of scour in shipwreck site formation processes and the preservation of wreck-associated scour signatures in the sedimentary record—evidence from seabed and sub-surface data. *Journal of Archaeological Science*, *33*(10), 1419–1432. https://doi.org/10.1016/j.jas.2006.01.011

Quinn, R., & Boland, D. (2010). The role of time-lapse bathymetric surveys in assessing morphological change at shipwreck sites. *Journal of Archaeological Science*, *37*(11), 2938–2946. https://doi.org/10.1016/j.jas.2010.07.005

Quinn, R., Bull, J. M., Dix, J. K., & Adams, J. R. (1997). The Mary Rose site-geophysical evidence for palaeo-scour marks. *International Journal of Nautical Archaeology*, *26*(1), 3–16. https://doi.org/10.1111/j.1095-9270.1997.tb01309.x

Quinn, R., Forsythe, W., Breen, C., Boland, D., Lane, P., & Omar, A. L. (2007). Process-based models for port evolution and wreck site formation at Mombasa, Kenya. *Journal of Archaeological Science*, *34*(9), 1449–1460. https://doi.org/10.1016/j.jas.2006.11.003

Quinn, R., & Smyth, T. A. G. (2018). Processes and patterns of flow, erosion, and deposition at shipwreck sites: A computational fluid dynamic simulation. *Archaeological and Anthropological Sciences*, *10*(6), 1429–1442. https://doi.org/10.1007/s12520-017-0468-7

Raineault, N. A., Trembanis, A. C., Miller, D. C., & Capone, V. (2013). Interannual changes in seafloor surficial geology at an artificial reef site on the inner continental shelf. *Continental Shelf Research*, *58*, 67–78. https://doi.org/10.1016/j.csr.2013.03.008

Scourse, J., Saher, M., Van Landeghem, K. J. J., Lockhart, E., Purcell, C., Callard, L., Roseby, Z., Allinson, B., Pieńkowski, A. J., O'Cofaigh, C., Praeg, D., Ward, S., Chiverrell, R., Moreton, S., Fabel, D., & Clark, C. D. (2019). Advance and retreat of the marine-terminating Irish Sea Ice Stream into the Celtic Sea during the Last Glacial: Timing and maximum extent. *Marine Geology*, *412*, 53–68. https://doi.org/10.1016/j.margeo.2019.03.003

Shchepetkin, A. F., & McWilliams, J. C. (2005). The regional oceanic modeling system (ROMS): A split-explicit, free-surface, topography-following-coordinate oceanic model. *Ocean Modelling*, *9*(4), 347–404. https://doi.org/10.1016/j.ocemod.2004.08.002

Sherwin, T. J. (1987). Inertial oscillations in the Irish Sea. *Continental Shelf Research*, *7*(2), 191–211. https://doi.org/10.1016/0278-4343(87)90079-3

Smyth, T. A. G., & Quinn, R. (2014). The role of computational fluid dynamics in understanding shipwreck site formation processes. *Journal of Archaeological Science*, *45*(1), 220–225. https://doi.org/10.1016/j.jas.2014.02.025

Soulsby, R. (1997). *Dynamics of marine sands: A manual for practical applications*. Thomas Telford.

Stieglitz, T. C., & Waterson, P. (2013). Impact of Cyclone Yasi on the wreck of the SS Yongala documented by comparative multibeam bathymetry analysis. *Queensland Archaeological Research*, *16*, 33. https://doi.org/10.25120/qar.16.2013.222

Stow, D. A. V., Hernández-Molina, F. J., Llave, E., Sayago-Gil, M., Díaz-del Río, V., & Branson, A. (2009). Bedform-velocity matrix: The estimation of bottom current velocity from bedform observations. *Geology*, *37*(4), 327–330. https://doi.org/10.1130/G25259A.1

Sumer, B. M. (2007). Mathematical modelling of scour: A review. *Journal of Hydraulic Research*, *45*(6), 723–735. https://doi.org/10.1080/00221686.2007.9521811

Sumer, B. M., & Fredsøe, J. (2002). *The mechanics of scour in the marine environment*. World Scientific.

Taormina, B., Percheron, A., Marzloff, M. P., Caisey, X., Quillien, N., Lejart, M., Desroy, N., Dugornay, O., Tancray, A., Carlier, A. (2020). Succession in epibenthic communities on artificial reefs associated with marine renewable energy facilities within a tide-swept environment. *ICES Journal of Marine Science*. https://doi.org/10.1093/icesjms/fsaa129

Tenzer, R., & Gladkikh, V. (2014). Assessment of density variations of marine sediments with ocean and sediment depths. *The Scientific World Journal*, *2014*, 9. https://doi.org/10.1155/2014/823296

Tomalin, D. J., Simpson, P., & Bingeman, J. M. (2000). Excavation versus sustainability in situ: A conclusion on 25 years of archaeological investigations at Goose Rock, a designated historic wreck-site at the Needles, Isle of Wight, England. *International Journal of Nautical Archaeology*, *29*(1), 3–42. https://doi.org/10.1006/ijna.2000.0285

Trembanis, A. C., Friedrichs, C. T., Richardson, M. D., Traykovski, P., Howd, P. A., Elmore, P. A., & Wever, T. F. (2007). Predicting seabed burial of cylinders by wave-induced scour: Application to the sandy inner shelf off Florida and Massachusetts. *IEEE Journal of Oceanic Engineering*, *32*(1), 167–183. https://doi.org/10.1109/JOE.2007.890958

UNESCO (2002) Convention on the Protection of the Underwater Cultural Heritage. In UNESCO (Ed.), *Records of the general conference: Resolutions* (31st session, Vol. 1, pp. 50–61). https://unesdoc.unesco.org/ark:/48223/pf0000124687.page=56

UNESCO (2017). The underwater heritage: Wrecks. http://www.unesco.org/new/en/culture/themes/underwater-cultural-heritage/underwater-cultural-heritage/wrecks/

Van Landeghem, K. J. J., Baas, J. H., Mitchell, N. C., Wilcockson, D., & Wheeler, A. J. (2012). Reversed sediment wave migration in the Irish Sea, NW Europe: A reappraisal of the validity of geometry-based predictive modelling and assumptions. *Marine Geology*, *295–298*, 95–112. https://doi.org/10.1016/j.margeo.2011.12.004

Van Landeghem, K. J. J., & Chiverrell, R. C. (2020). Bed erosion during fast ice streaming regulated the retreat dynamics of the Irish Sea Ice Stream. *Quaternary Science Reviews*, *245*, 106526. https://doi.org/10.1016/j.quascirev.2020.106526

Van Landeghem, K. J. J., Uehara, K., Wheeler, A. J., Mitchell, N. C., & Scourse, J. D. (2009). Post-glacial sediment dynamics in the Irish Sea

and sediment wave morphology: Data-model comparisons. *Continental Shelf Research*, *29*(14), 1723–1736. https://doi.org/10.1016/j.csr.2009.05.014

Van Landeghem, K. J. J., Wheeler, A. J., Mitchell, N. C., & Sutton, G. (2009). Variations in sediment wave dimensions across the tidally dominated Irish Sea, NW Europe. *Marine Geology*, *263*(1–4), 108–119. https://doi.org/10.1016/j.margeo.2009.04.003

Vanninen, P., Östin, A., Bełdowski, J., Pedersen, E. A., Söderström, M., Szubska, M., Grabowski, M., Siedlewicz, G., Czub, M., Popiel, S., Nawała, J., Dziedzic, D., Jakacki, J., & Pączek, B. (2020). Exposure status of sea-dumped chemical warfare agents in the Baltic Sea. *Marine Environmental Research*, *161*, 105112. https://doi.org/10.1016/j.marenvres.2020.105112

Walbridge, S., Slocum, N., Pobuda, M., & Wright, D. J. (2018). Unified geomorphological analysis workflows with Benthic Terrain Modeler. *Geosciences*, *8*(3), 94. https://doi.org/10.3390/geosciences8030094

Wang, X. L., & Swail, V. R. (2001). Changes of extreme wave heights in northern hemisphere oceans and related atmospheric circulation regimes. *Journal of Climate*, *14*(10), 2204–2221.

Ward, I. A. K., Larcombe, P., & Veth, P. (1999). A new process-based model for wreck site formation. *Journal of Archaeological Science*, *26*(5), 561–570. https://doi.org/10.1006/jasc.1998.0331

Ward, S. L., Neill, S. P., Van Landeghem, K. J. J., & Scourse, J. D. (2015). Classifying seabed sediment type using simulated tidal-induced bed shear stress. *Marine Geology*, *367*, 94–104. https://doi.org/10.1016/j.margeo.2015.05.010

Wessel, P. (1998). An empirical method for optimal robust regional-residual separation of geophysical data. *Mathematical Geology*, *30*(4), 391–408. https://doi.org/10.1023/A:1021744224009

Wessex Archaeology. (2005). *Strategic Environmental Assessment Sea 6: Irish Sea. Maritime Archaeology*. https://assets.publishing.service.gov.uk/government/uploads/system/uploads/attachment_data/file/197296/SEA6_Archaeology_Wessex.pdf

Westley, K., Plets, R., Quinn, R., McGonigle, C., Sacchetti, F., Dale, M., McNeary, R., & Clements, A. (2019). Optimising protocols for high-definition imaging of historic shipwrecks using multibeam echosounder. *Archaeological and Anthropological Sciences*, *11*, 3647–3648. https://doi.org/10.1007/s12520-019-00831-6

Westley, K., Quinn, R., Forsythe, W., Plets, R., Bell, T., Benetti, S., McGrath, F., & Robinson, R. (2011). Mapping submerged landscapes using multibeam bathymetric data: A case study from the north coast of Ireland. *International Journal of Nautical Archaeology*, *40*(1), 99–112. https://doi.org/10.1111/j.1095-9270.2010.00272.x

Wheeler, A. J. (2002). Environmental controls on shipwreck preservation: The Irish context. *Journal of Archaeological Science*, *29*(10), 1149–1159. https://doi.org/10.1006/jasc.2001.0762

Whitehouse, R. J. S. (1998). *Scour at marine structures: A manual for practical applications*. Thomas Telford. https://doi.org/10.1680/sams.26551

Whitehouse, R. J. S., Harris, J. M., Sutherland, J., & Rees, J. (2011). The nature of scour development and scour protection at offshore windfarm foundations. *Marine Pollution Bulletin*, *62*(1), 73–88. https://doi.org/10.1016/j.marpolbul.2010.09.007

Woods, M. A., Wilkinson, I. P., Leng, M. J., Riding, J. B., Vane, C. H., Lopes dos Santos, R. A., Kender, S., De Schepper, S., Hennissen, J. A. I., Ward, S. L., Gowing, C. J. B., Wilby, P. R., Nichols, M. D., & Rochelle, C. A. (2019). Tracking Holocene palaeostratification and productivity changes in the Western Irish Sea: A multi-proxy record. *Palaeogeography, Palaeoclimatology, Palaeoecology*, *532*, 109231. https://doi.org/10.1016/j.palaeo.2019.06.004

SUPPORTING INFORMATION

Additional Supporting Information may be found online in the supporting information tab for this article.

How to cite this article: Majcher J, Quinn R, Plets R, et al. Spatial and temporal variability in geomorphic change at tidally influenced shipwreck sites: The use of time-lapse multibeam data for the assessment of site formation processes. *Geoarchaeology*. 2021;36:429–454. https://doi.org/10.1002/gea.21840